A NOVEL TECHNIQUE FOR ECG DENOISING

DISSERTATION

SUBMITTED IN PARTIAL FULFILLMENT OF THE REQUIREMENTS
FOR THE AWARD OF THE DEGREE
OF

MASTER OF TECHNOLOGY
IN
SIGNAL PROCESSING & DIGITAL DESIGN

Submitted by:

AKSHAY KUMAR SHARMA

2K12/SPD/02

Under the supervision of

Shri M.S. Chaudhary
(Associate Professor, E&C)

DEPARTMENT OF ELECTRONICS & COMMUNICATION ENGINEERING
DELHI TECHNOLOGICAL UNIVERSITY
(Formerly Delhi College of Engineering)
Bawana Road, Delhi-110042

2014

CERTIFICATE

DELHI TECHNOLOGICAL UNIVERSITY,
(Formerly Delhi College of Engineering)
BAWANA ROAD, DELHI – 110042
Department of Electronics & Communication Engineering

This is to certify that the thesis titled **"A Novel Technique for ECG Denoising"** submitted by Akshay Kumar Sharma, Roll. No. 2K12/SPD/02, in partial fulfillment for the award of degree of Master of Technology in Signal Processing & Digital Design at **Delhi Technological University, Delhi**, is a bonafide record of student's own work carried out by him under my supervision and guidance in the academic session 2013-14. The matter embodied in dissertation has not been submitted for the award of any other degree or certificate in this or any other university or institute.

(Shri M.S. Chaudhary)

ASSOCIATE PROFESSOR
Department of Electronics & Communication Engineering
Delhi Technological University,
(Formerly Delhi College of Engineering)
Delhi -110042

ACKNOWLEDGEMENT

I express my sincere gratitude to my guide **Shri M.S. Chaudhary** for giving valuable suggestion during the course of the investigation, for his ever encouraging and moral support. His enormous knowledge and investigation always helped me unconditionally to solve various problems. I would like to thank him for introducing me with the problem and providing valuable advice throughout the course of work. I truly admire his depth of knowledge and strong dedication to students and research that has made him one of the most successful professors ever. His mastery of any topic is amazing, but yet he is such a humble and down to earth person. I am glad that I was given opportunity to work with him. He surely brings out the best in his students.

I am greatly thankful to **Prof. Rajiv Kapoor, Professor and Head,** Department of Electronics & Communication Engineering, entire faculty and staff of electronics & Communication Engineering for their, continuous support, encouragement and inspiration in the execution of this "**thesis"** work.

I would like to thank my parents who bestowed upon me their grace and were source of my inspiration and encouragement.

I am thankful to almighty god his grace and always with me whenever I felt lonely.I am also thankful to my friends for their continious support and helpfullness whenever it is needed.

Akshay Kumar Sharma

ABSTRACT

The Electrocardiogram is the record of the electrical activities of the heart. During the acquisition process of the cardiac signal, several noises are added to the signal, making the medical diagnosis of this critical signal difficult. Important noises induced in the signal are: power line interference, baseline wander and electromyography noise. In the case of exercise electrocardiogram, baseline wander noise is naturally present.

Several works has been done in the field of noise cancellation in cardiac signals. In this thesis work, a novel approach for the removal of baseline noise has been implemented by using the hybrid of morphological filters and empirical mode decomposition technique. The proposed algorithm has been made partially adaptive to the variations of the heart rate. As, the heart rate increases, there are definite changes in the morphology of the characteristic waves of the heart signal. Thus it becomes essential to make the denoising specially in the case of baseline drift noise adaptive to these variations when using morphological filters. The results of the proposed algorithm are compared to the existing techniques and are found to perform better.

TABLE OF CONTENTS

LIST OF FIGURES

LIST OF TABLES

LIST OF ABBREVIATIONS

ECG	Electrocardiogram
EMG	Electromyography
BW	Baseline Wander
DWT	Discrete Wavelet Transform
EMD	Empirical Mode Decomposition
MO	Morphological Operations
ECGIDDB	ECG-ID Database
SNR	Signal to Noise Ratio
MSE	Mean Square Error
HT	Hard Thresholding
ST	Soft Thresholding
SE	Structuring Element

Chapter 1

INTRODUCTION

Noise removal in medical signals is of vital importance and special care and caution should be observed in the process, since medical diagnosis is affected by the operations performed on the signal. Hence, losing an important information content in the process of denoising can adversely affect the diagnosis step.

Electrocardiogram is nearly a quasi-periodic signal which measures the electrical activities of heart and thus give the details of the underlying physiology of the heart. Heart generates electrical waves in the process of depolarization and repolarization of certain cells because of the motion of Na^+ and K^+ ions in blood. The ECG signal information content is mostly present in a frequency band of 0.5Hz to 120 Hz [1]. The ECG signal is acquired by placing the electrodes at standard locations usually chest, arms and legs on human body [2]. If any subject is suffering from any cardiac arrhythmia, it is reflected in its ECG in the form of altered morphology of electrocardiogram. There are five important characteristic waves present in an ECG signal which reveals the state of heart namely P wave, QRS complex, S wave, T wave and U wave [1]. There amplitude, location and duration are of much clinical importance and should be preserved from any sort of noise and distortion.

1.1 Scope of Work

At the time of ECG signal acquisition different type of noises are introduced, corrupting the signal. Denoising of the ECG signal, thus becomes critical for proper medical diagnosis of the ECG. Thus the scope of this thesis work is limited to the denoising aspects of the ECG signal. One important factor related to the denoising concept is, the morphology of ECG signal. The characteristic waves embedded in the signal varies to a large extent in their shape, size and location and preserving there morphology is another key point, must be ensured for successful denoising. Software based analysis has thus gain high popularity. Thus this work covers an exhaustive study of the denoising algorithms with their advantages and limitations. Wavelets is emerging as an important tool in denoising, hence a comprehensive study of wavelets for ECG denoising has been

included in the work. This work is referred as the background work and comprehensive results of this work has been included in the Appendix, for easy reference.

Another major issue at the time of ECG signal acquisition is the interference of a low frequency noise referred as Baseline Drift noise. The main motive of this work is the correction of this baseline noise by a proposed novel algorithm. All the basics of the hybrid technique has been discussed in detail while the course of this thesis. Lastly, detailed and exhaustive results with conclusive remarks has been taken up which validates the performance efficiency of the proposed algorithm.

1.2 Generation of Electrocardiogram

There are cardiac tissues that are excited on their own resulting into contraction without any command from the nervous system. They are responsible for generation of electrical impulses. Sinoatrial node or SA node, can be regarded as the natural pacemaker of the heart. Electrical impulses are generated at SA node and grows over the left and right atria in order to contract it, known as atrial depolarization. After the atrial depolarisation is initiated, the atrium begins to contract and the blood is emptied into ventricles before the electrical impulse reaches the Atrioventricular node (AV node). Then the impulse from AV node travels to Purkinje fibres with a natural delay of 0.1 seconds. Strong electrical impulse is generated by Purkinje fibres which empties the blood from the ventricles. The delay of 0.1 seconds ensures that the blood is completely drained from the atria before the ventricular contraction. The contraction is succeeded by ventricular repolarization, a recovery process where the previously excited cells are restored. A fraction of the electrical potential also flows to the surface of body. With the application of electrodes on the skin at some particular selected points, the potential can be captured as an ECG signal [3].

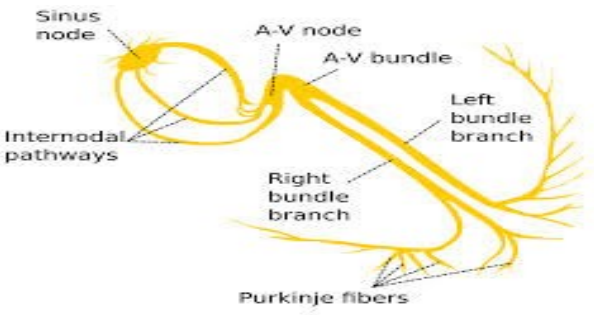

Fig 1.1: Indicative electrical activities of heart.

1.3 Structure of Electrocardiogram

To be able to denoise ECG signal properly, it is critical to be equipped with the knowledge of ECG morphology. ECG waveform of a healthy subject comprises of five characteristic morphologies: P wave, ST segment, U wave, QRS complex and T wave. Figure below depicts a normal ECG:

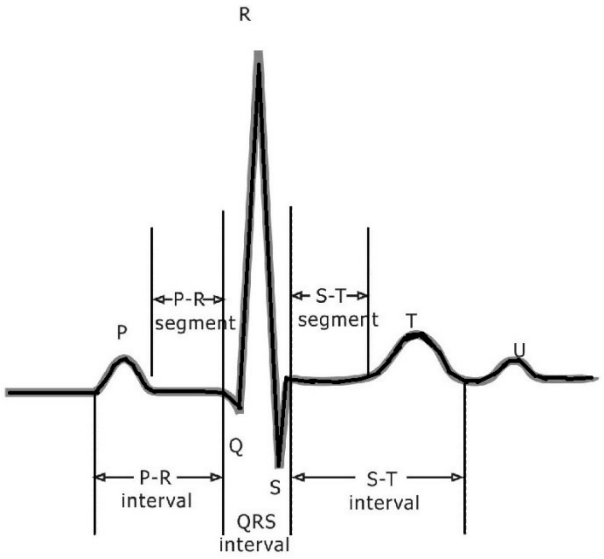

Fig 1.2: A normal ECG with its components

P wave: It occurs at the time of depolarization of atria. Depolarization of atria occurs when the conduction of electrical impulse takes place from SA node to the AV node and the electrical impulse spreads from the right atrium to the left atrium.[20]

QRS complex: this is the most distinctly visible wave of all. The QRS complex comprises of three constituent waves as: Q, R and S wave. This complex is a result of depolarization of the both ventricles. The ventricles muscles are much heavier and has larger mass, therefore a large potential is generated for contraction and hence a large amplitude QRS complex is formed.

T wave: T wave and the initial segment of ST are a result of Ventricular repolarization.

U wave: U wave is hardly seen and its origin is not clear.

The amplitude, duration and the characteristic property has been discussed in the table 1.1 for easy reference.

Table 1.1 Characteristics of important Electrocardiogram morphology

Characteristic Feature	Illustration	Magnitude (in mV)	Duration (in ms)
P wave	Due to depolarization of atrial	0.1 - 0.2	80
PR interval	Time taken by the electrical impulse to reach from SA node to the ventricles via AV node	-	120 - 200
QRS complex	Due to ventricle depolarization	1 – 1.2	80 – 120
J point	Denotes the end of QRS complex	-	-
ST interval	Denotes the time period for the depolarization of ventricles		80 – 120
T wave	Due to ventricle repolarization	0.12 - 0.3	160
QT interval	Time period marked from the starting of the QRS complex to the end of T wave. As the heart rate (i.e. heart beat per minutes) increases, the QT interval shortens.	-	300-430
RR interval	Time period between two consecutive R peaks. This is also a measure of the heart rate.	-	0.2-1.2

1.4 Artifacts in ECG

Many sorts of artifacts can be added to the ECG signal at the time of signal acquisition. This corrupts and disturbs the measurements in ECG. Among all, the noises of primary interest are:

1. Power line interference,
2. EMG noise (wideband stochastic noise), and
3. Baseline interference.

Though the noises are classified into further more types as described in the figure below, but these three can sufficiently represents the effect of all other noises. They are discussed in detail. The following figure is self-explanatory, depicting different noise sources:

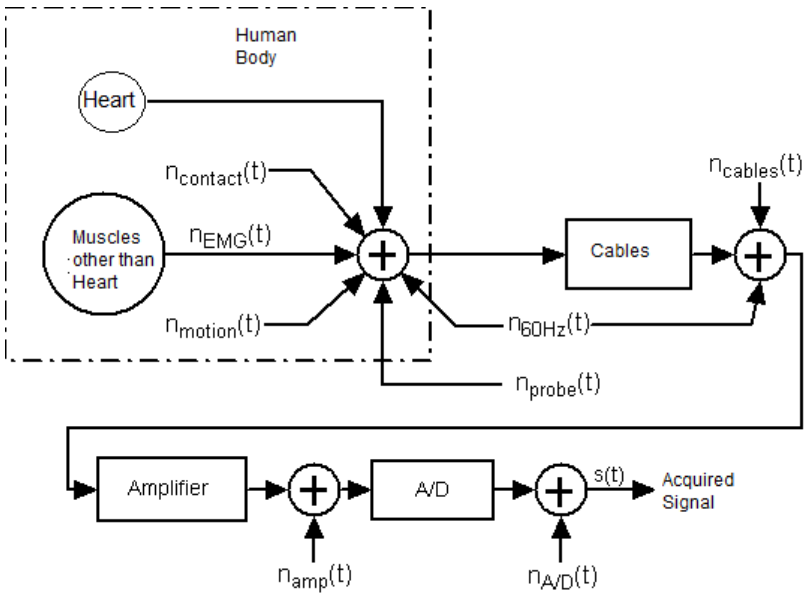

Fig. 1.3: Principal noise sources in ECG

1.4.1 Power Line Interference

Power line noise interference occurs due to inductive or capacitive coupling between the two circuits, the ECG acquisition circuit and the circuit used to feed the power to the device. This introduces the frequency band of the power supply in the ECG signal which is 50/60 Hz and its harmonics. Thus, the power line noise can be modeled as:

$$n_{60}(t) = Asin(2\pi.60.t + \varphi) \tag{1.1}$$

The average value of A is a function the amount of coupling between the power lines and the acquisition equipment. The phase, represented by φ in the above equation is a random variable whose value varies in the band $[-\pi, \pi)$. Plotting the power spectrum of an ECG corrupted by power line noise clearly reveals the presence of a noise component of 60Hz as depicted in the graph below:

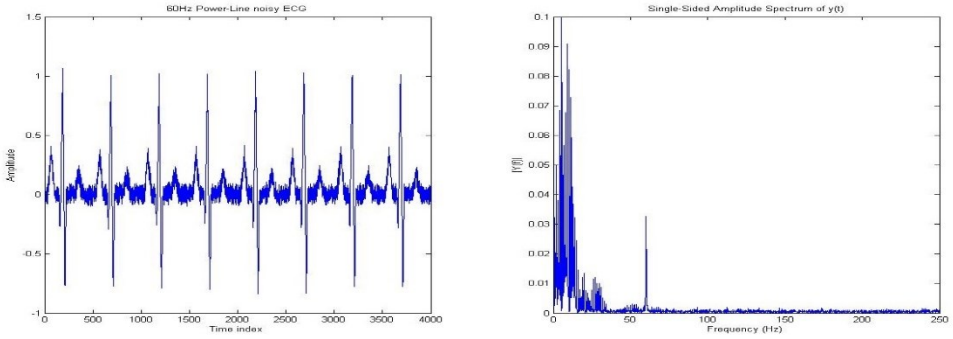

Fig 1.4: Power line corrupted noisy signal with its magnitude spectrum.

1.4.2 Electromyography noise (EMG)

Unintended capturing of the signal potential from muscles other than heart interferes in the frequency band of the ECG signal and hence corrupts the signal with noise. This noise is referred as EMG noise. The fraction of the crosstalk introduced in the signal is subject to the amount of movement of muscles in the vicinity of the electrodes. EMG noise is random noise and Gaussian distribution function can be used to model the noise. While the mean of the distribution can be assumed to be at zero but the variance of the distribution varies as a function of the environmental variables such as quality of probes, positioning of probes etc. Studies conforms that the maximum amplitude of the EMG noise is typically 10% of the maximum peak to peak amplitude of the signal.

Amplitude ~ 10% of peak amplitude of ECG

Frequency ~ broadband (20 – 1000 Hz)

Many other noise sources such as *instrumentation noise* and *contact potential noise* have very much similar characteristics to that of EMG noise.

Instrumentation Noise: the electrical instruments used for the acquisition of ECG signal such as analog to digital converter, amplifier, cables and electrode probes contributes to noise.

Electrode contact noise: caused due to imperfect positioning of the electrode probes and due to poor impedance matching of the electrodes.

The frequency characteristics and the nature of this noise is very similar to that of EMG noise and hence are not taken up separately.

1.4.3 Baseline Wander (Motion Artifact)

Baseline wander or baseline drift noise is a low frequency noise introduced into the ECG signal due to movement because of respiration. In the process of respiration, the diaphragm moves up and down, hence the baseline of the ECG signal gets disoriented. Other possible causes of baseline drift includes movement and vibrations at the time of signal acquisition. This noise introduces an unusually low frequency into the ECG signal usually below 1 Hz.

1.5 Organization of the Thesis

The thesis has been segmented into five chapters as described below:

Chapter 2: in this chapter an exhaustive study of the existing algorithms for ECG signal denoising has been done.

Chapter 3: this chapter presents the proposed algorithm in a detailed manner. First the basics for the proposed algorithms are explained followed by a comprehensive flow chart of the proposed algorithm.

Chapter 4: the results and associated discussions are presented in this chapter.

Chapter 5: final conclusions and future scope of the proposed algorithm are discussed in detail in this chapter.

Chapter 2

ECG DENOISING ALGORITHMS

This chapter discusses about different denoising algorithms present in the Literature for noise removal in ECG signals. There advantages and limitations have been discussed in detail. A thorough study of the Literature reveals growing attention towards the wavelet transforms for the purpose of denoising. Hence, an exhaustive comparative study was carried out to study the noise removing capabilities of the wavelets for ECG signals. Also, since QRS detection has been used in the proposed algorithm, hence a brief overview of the detection techniques are covered in a later section.

2.1 Literature Review

From the past several years, constant efforts have been made in the field of denoising, beat detection (QRS detection), classification and signal compression of the cardiac signal. Most of the denoising algorithms can be classified on the basis of the domain information they utilise for the purpose of denoising i.e. Denoising algorithms based on time domain representation and denoising algorithms based on frequency domain representation of the ECG waveform. Wavelets utilises both the frequency domain and time domain information thus is studied under separate head. Algorithms concerning with the denoising of Baseline drift noise has been studied under another section.

In the research paper by S.K. Jagtap *et al.*, [4] window based, low pass and high pass FIR filters have been implemented using Kaiser, Hanning, Hamming and Rectangular windows for reduction of noise in ECG signals. Filter order of 100 was used. The performance was analysed by comparing the power of the signal before filtration and after the filtration. The FIR filter with this order, using rectangular window has ripples in the pass and stop bands and has sharp attenuation at the transition frequency. Phase response of the rectangular window was found to be linear and in comparison to other filters, this filter is more stable. In 2010, K.L. Yadav *et al.* used adaptive algorithms i.e. RLS and LMS for denoising of ECG signals in their paper [5]. It was concluded in their paper, that the adaptive filter using RLS algorithm performs better compared to others.

In the paper by M.Z.Rahman *et al.* [6] simple sign based adaptive filters are used for removing the noise from ECG signals which have an advantage of being computationally inexpensive. The proposed algorithm performs better in applications like biotelemetry. The performance of adaptive algorithms for noise removal has been compared by C.H. Chang *et al.* in their paper [7]. The study in this paper reveals that the adaptive filter with reference is not very effective for noise cancellation since the reference signal is not correlated well enough with the noise components in the primary input.

There are many other approaches in the literature developed so far for the task of denoising. Initial efforts for denoising of ECG used the concepts of Linear Filters and Adaptive Filters [8][9][10] and lately Kalman Filter [11] but all had some added disadvantages like that of poor performance in case of FIR filter, minimum error constraint in adaptive filters. Fuzzy logic [12] when used for denoising had limitation in concern with its membership function. Some Statistical techniques such as independent component analysis [13], [14] (ICA), principal component analysis [15] (PCA), and neural networks [16] have been implemented for denoising of an ECG signal.

2.2 Wavelets for ECG signal Denoising – Background Work

Recent developments in past, introduced WTs as an effective tool to deal with such non-stationary signals and complex stochastic noise process. The denoising with wavelet transforms, initially proposed by Donoho *et al*. [17], is carried forward to the field of ECG denoising and recently many algorithms [18][19][20] are built over it.

To study the denoising capability and efficiency of wavelet transforms an exhaustive study was carried out to determine the optimize solution for wavelet and thresholding for each of the three major type of noises using five different thresholding techniques (viz. Hard thresholding, Soft thresholding, Semi-soft thresholding, Stein thresholding and Neighbourhood thresholding) and ten different wavelet functions. The functions chosen are such that there physical properties maximally resembles with that of ECG, so that better denoising results are obtained. These results provides an exhaustive comparative study of the denoising performance by wavelet in all domains and thus can prove to be critical when developing any hybrid model for denoising. The denoising method using the WTs comprises of three basic steps: First, performing forward WT and extracting the wavelet coefficients. Second is the 'Shrinkage step', where threshold and shrinking

operation is performed on the extracted coefficients in accordance with the defined technique. Third step involves taking the inverse wavelet transform.

The five different thresholding techniques being used in the work are discussed. Thresholding is usually applied only on the detailed coefficients because approximation coefficients contains low frequency components and are least affected by noise. Let *d* represent a single detail wavelet coefficient and $S^{\lambda}(.)$ represents *Shrinkage function* for λ threshold level [21].

A. Hard Thresholding

$$S^{\lambda}(d) = d.(abs(d) > \lambda) \tag{2.1}$$

B. Soft Thresholding

$$S^{\lambda}(d) = \begin{cases} sign(d)(|d| - \lambda); |d| \geq \lambda \\ 0; \quad |d| < \lambda \end{cases} \tag{2.2}$$

C. Semi-Soft Thresholding

$$S^{\lambda\lambda^1}(d) = \begin{cases} 0; \quad |d| \leq \lambda \\ sign(d)\frac{\lambda^1(|d|-\lambda)}{\lambda-\lambda^1}; |d| \geq \lambda \\ d; \quad |d| > \lambda^1 \end{cases} \tag{2.3}$$

Where, $\lambda^1 = \lambda \times \mu$, while μ is chosen on the basis of experimental results. In this paper, μ is taken as 1.8 for baseline noise and 1.2 for powerline and wideband noise. If $\mu = 1$; it becomes hard thresholding and if $\mu = \infty$; it becomes equivalent to soft thresholding [22].

D. Stein Thresholding

Stein thresholding is achieved by squaring the scaled soft thresholding coefficients, thus making the transition much more gradual.

E. Neighbouring Coefficients with Level Dependent Threshold Estimator (NE)

This threshold estimator involves the neighbouring coefficients also, while determining the threshold function. Here, the single wavelet coefficient is assumed to be modified as:

$$D_k^2 = d_{k-1}^2 + d_k^2 + d_{k+1}^2 \tag{2.4}$$

So, that effect of two of the neighbouring coefficients is taken into account. Now the shrinkage function is given as [7]:

$$S^{\lambda}(d_k) = \begin{cases} d_k = 0;\ D_k^2 \ \leq\ \lambda^2 \\ d_k = d_k(1 - \frac{\lambda^2}{D_k^2})\ ;\ D_k^2 \ >\ \lambda^2 \end{cases} \tag{2.5}$$

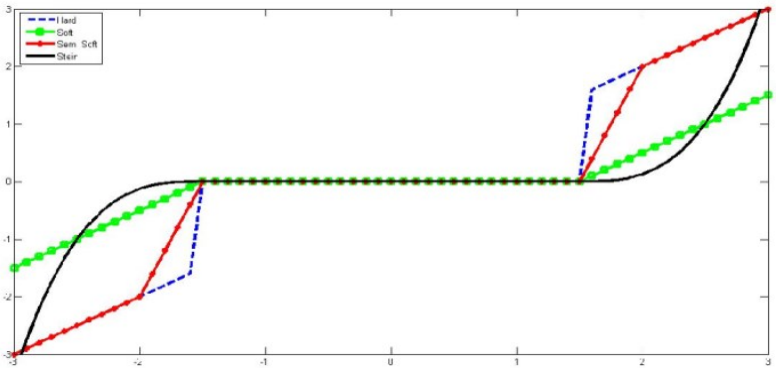

Fig.2.1 Wavelet Shrinkage functions for different types of thresholding techniques

A. Removal of EMG/wideband stochastic noise

The whole process can be summarized in the following steps:-

Step1: Decomposition of the noisy ECG signal is done into the wavelet coefficients using the wavelet decomposition tree. Any of the wavelet can be chosen from the wavelet family for this purpose.

Step 2: From the obtained wavelet coefficients the noise variance is estimated and thus threshold level λ is estimated using the universal threshold formulae as discussed earlier.

Step 3: Then the different thresholding schemes are implemented and finally modified coefficients are reconstructed using the IDWT.

B. Removal of Baseline Drift

Among the many proposed algorithms [24] for removal of baseline drift noise, in this paper the adopted algorithm [25] is based on wavelet approach for baseline wander suppression. This noise constitutes a frequency band of 0-0.5 Hz and thus for the purpose of denoising following steps are performed:-

Step1: **S**ignal is decomposed in a way that the final level of the approximation coefficients represents a frequency band of 0-0.5 Hz.

Step2: The noise variance is then estimated from this very level of the decomposed coefficients. For a 1 KHz signal, at a scale of 2^8, the approximation coefficient represents a frequency band of 0-0.5 Hz.

Step3: These coefficients are modified in accordance with the thresholding scheme.

C. Removal of Power Line Interference (PLI)

The power-line signal is a narrow-band signal. For removing the PLI, whole process can be summarized in the following steps:-

Step1: The noise is estimated using the *2^{nd} level wavelet coefficients* that correspond to the frequency band of this signal (50/60 Hz).

Step2: Once the signal noise estimation is done, the threshold value is estimated and further the detailed coefficients are modified accordingly.

Step3: The updated wavelet coefficients are then reconstructed to give the denoised signal.

The results of this work has been compiled in the Appendix I. Very exhaustive results are presented which gives the optimized solution for each type of noise. These results are fruitful and valuable for developing any hybrid algorithm using wavelets. While removing Baseline wander noise using wavelet, little fluctuations are noticed in the results when the frequency of the baseline noise is varied thus conforming to the study of D.T. Luong *et al.* [26]. The denoising performance varies with different wavelet functions used.

2.3 Baseline Noise Removing Algorithms

In this section, a survey of the algorithms developed so far for the removal of baseline noise has been done. Though baseline noise has got little attention when compared to other noises, all the important work has been organised here with brief description of the algorithm and its limitations. Wavelets has been found ineffective for the removal of baseline noise as is confirmed in the study by Luong *et al*. [26]. Thus, baseline noise removal algorithms using empirical mode decomposition and morphological operators has been discussed in the following two sections.

2.3.1 Denoising by EMD and associated Hybrid Techniques

Empirical mode decomposition is a very good signal filtering technique as exploited in the paper by Boudraa *et al.* in [27]. EMD finds many applications for denoising of the ECG signals. This can be attributed to the characteristic properties of the decomposed Intrinsic Modes which are a function of the local variance of the signal and hence proper decomposition of the signal is possible. Cardiac signal being non-stationary in nature, EMD is the best tool available to deal with such signals so far. Though many works have been done for denoising of ECG signal using EMD but relatively very low attention has been given in removing the low frequency noise/baseline noise.

High frequency noise removal by EMD and hybrid techniques has been successfully done in many research works as discussed subsequently. Denoising of ECG signal using linear filtering [28] (Butterworth Low pass filter) gives improved result when compared to direct denoising by EMD method. Denoising of ECG signal by EMD combined with Adaptive Filtering gives better results as compared to the EMD with linear filtering techniques as the filter coefficients are adaptively derived in this case. Model based denoising [29] of ECG signal using EMD is a better denoising technique when compared to other techniques as it helps preserving the sharp edges, transitions and the QRS complex by fitting the modelled ECG to the noisy ECG. ECG denoising using EMD and Wavelet [30] is a very effective technique for denoising of ECG signal. To improve on this method another modification is done by Zhang *et al.* in [31]. This method analyses the Energy of each IMF and accordingly detects the noisy IMFs and thus only the noisy IMFs are denoised using Wavelet Soft thresholding Technique. This reduces the computation cost as well and thus is the better technique till now. The limitation of all the above described methods is that none of the method deals with removing of the baseline drift noise, since all these methods are processing lower order IMFs which basically contains high frequency components and higher order IMFs containing low frequency/baseline noise components are left untouched.

In the paper by Zhi-Dong Zhao *et al.*, [32] titled, "A New Method for Removal of Baseline Wander and Power Line Interference in ECG signals" first time EMD was used for removing of Baseline Noise. In this paper, the residue signal was regarded as an estimate of the Baseline noise and is removed to correct the noise signal.

In the paper titled, "Accurate Removal of Baseline Wander in ECG Using Empirical Mode Decomposition" by Na Pan *et al.* [33] the signal used is decomposed into 15 IMFs and the last 3 IMFs are said to be comprising of mostly Baseline Noise components. Thus denoised signal is reconstructed by eliminating the last 3 IMFs.

Limitations and Scope: only one particular ECG signal was used which was decomposed into 'n' number of IMFs, and all discussions are carried out on that particular signal. While the decomposition process by EMD is a function of the sampling frequency and the amount of variations. Therefore, a rigid mechanism should be defined for selecting the number of IMFs to be selected. EMD alone does not possess strong denoising capabilities and hence should be combined with some other technique to fetch optimum results.

2.3.2 Denoising by Morphological Operators

In the paper by Chee-Hung *et al.* [34] titled, "Impulsive noise suppression and background normalization of electrocardiogram signals using morphological operators", morphological operation was adopted first time for removing baseline wander from a biomedical signal. The signal used was an EKG signal for the analysis. First a triangular shaped structuring element was used and then experiments were carried out with a parameterized structuring element with a dome like structure having parameters as width, height and shape. Analysis were done to optimize the parameters of the structuring element.

Limitations: ECG signal morphology is quite different from that of ECG signals. Hence the algorithm needs to be modified in accordance to the morphology of the ECG signal before applying.

In the paper titled, "A Morphology based algorithm for baseline wander elimination in ECG records", by OGUZ *et al.* [35] opening operation is followed by closing. The opening operation was used for removing the positive pulses i.e. P, R, T and U waves while the closing operation was used to extract the negative pulses i.e. Q and S wave. In this paper, a disk shaped structuring element was used. The opening operation was performed prior to the closing operation since the closing operation if would have been performed before, could have filled the negative valleys present between P and R pulse and R and T pulse.

Limitations: an ECG like, but not pure ECG signal was used for the analysis purpose where the morphology of the used signal is different from the original signal. Thus, the defined SE are not good approximate for a real ECG. A disk shaped SE was used without any evidence.

In another paper by P. Sun *et al.* in [36], "An Improved Morphological Approach to Background Normalization of ECG Signals", neonatal ECG signal was picked up for analysis. ECG signals of neonatal have a characteristic slope in QT segment. This paper specifically aims at preserving the QT interval. In this work opening and closing operations are used in tandem and then the average is taken. In this work, first the QRS complex is removed from the ECG signal. Then QT segment is estimated with the help of Bazett's correction and is set as the structuring element for the second set of morphological filtering. A linear structuring element is used.

Limitations and Scope: this paper specifically deals with only the ECG signals of neonatal which cannot be generalized to other ECG signals. Hence, a much more generalize approach can be developed which can adapt to the changes in the signal.

In a recent paper by Zhongguo Liu *et al.* [37], "ECG Signal Denoising Based on Morphological Filtering", the morphologies present in ECG are removed in two steps by using opening and closing operations in tandem and then taking the average. First, the QRS complex is removed and in second step the P and T pulses are removed. Linear structuring elements are set in accordance with the available biological data.

Limitations: ECG being a quasi-periodic and dynamic signal, the pulse width is not fixed hence a much more comprehensive and adaptive structuring element should be formed.

2.4 Motivation for Proposed Work

In spite of recent development in the field of ECG signal denoising, baseline noise removal has always been a weak link. The noise adds heavy distortion to the signal and makes proper diagnosis of the signal difficult. Hence, it becomes very important to properly correct the baseline of the signal. Thus, there is a desperate need for devising such an algorithm. Another key motivating factor for this work is the normal changes observed in the Exercise ECG [38] recorded at high levels of heart rate. There is an inherent baseline drift, an upward slope in the ST interval as the heart rate increases and none of the baseline correction algorithms deals with this problem. Keeping this in mind,

a novel technique for baseline noise removal has been proposed which has better performance when compared to other denoising algorithms available and is also adaptive to the changes in heart rate. The proposed algorithm successfully overcomes the shortcomings of the empirical mode decomposition and the morphological operations to tackle the baseline noise. The limitation of EMD has been excelled by the use of Hybrid technique. A defined criterion has been formulated to identify and remove the number of IMFs corrupted by the baseline noise which was missing in the earlier algorithms proposed so far. Morphological operators has been merged with EMD technique, which gave good results in comparison to the available algorithms. The limitation concerning with setting the structuring element of morphological filters for ECG signal has also been looked after by taking a data driven structuring element. A little literature review for QRS complex detection algorithms has been carried out in the next section.

2.5 Review of QRS Complex detection Algorithms

QRS complex detection in ECG signals has always been an absorbing topic for researchers. Numerous algorithms such as derivative based algorithm [39][40]; algorithm based on Digital filters [41] [42]; Wavelet based QRS detection algorithm[43]; Singularity detection based algorithms [44]; QRS detection algorithm based on local maxima [45]; Filter bank Methods [46]; Neural network approaches; adaptive filters ; Hidden Markov Models[47]; Mathematical morphology based algorithms [34]; Genetic Algorithms; Hilbert Transform based QRS detection [48]; Zero-crossing based QRS detection, etc. are present in the literature all having their share of advantages and limitations . An exhaustive survey and comparative study of all the QRS detection algorithms has been done in the paper titled, “The Principles of Software QRS Detection”, by B.U. Kohler *et al.* [49].

Chapter 3

NOVEL TECHNIQUE FOR BASELINE REMOVAL IN ECG

In this section, a new approach developed for the removal of Baseline Wander noise in ECG signal is discussed. As mentioned before, Baseline drift is a low frequency noise and its removal is an important task for proper diagnosis of the signal. The algorithm is a hybrid of Empirical Mode Decomposition (EMD) and Morphological filters. The baseline corrupted ECG signal is first decomposed into its constituent IMFs and residue. The higher order IMFs broadly represents the low frequency components (i.e. the baseline noise) of the corrupted ECG. Thus a new ECG signal is reconstructed after removing the baseline corrupted higher order IMFs using EMD but the baseline noise removal capability of EMD is not very strong and hence the newly derived signal is subsequently given as input to the morphological filters. While the Structuring Element (SE) for the morphological filters is made to be partially adaptive and is derived from the data itself (for the II phase of filtering), making the algorithm robust against variations in the R-R interval due to change in the heart rate. Mild variations in R-R interval are observed from one subject to another while strong variations are observed in case of any arrhythmia, also high heart rates are observed in case of exercise ECGs. Therefore building a data driven 'SE' can prove to be a vital step for ECG signal denoising. In upcoming sections, first a detailed description of EMD, Morphological filters and the QRS complex detection algorithm is given followed by the algorithm flow chart which summarizes the complete picture of the method.

3.1 Empirical Mode Decomposition

As per the study of Huang et al. (1998, 2001), incomplete, distorted and false results may come up when standard Fourier-based applications are used with non-stationary and non-linear signals. To manage such signals better, Huang presented Empirical Mode Decomposition (EMD), where the signal is decomposed into its constituent intrinsic mode functions (IMFs). These IMFs are symmetric, mono components derived from the initial compound components of the signal. The IMFs generates instantaneous frequencies as a function of time and thus enhances the identity of the imbedded

information at different frequency levels.

In EMD, the decomposition step depends upon the local characteristic time scale of signal thus making it durable for non-stationary and non-linear signals. By using the local characteristic time scales, the embedded oscillatory modes of the signal are identified. Thus EMD emerges as a strong adaptive data processing technique for IMF extraction and the major benefit of using EMD is that the basis functions used for decomposition of the signal are not predefined but are adaptively derived from the signal itself and hence EMD finds special applications for signals like ECG which are non-stationary in nature.

IMFs characterize the oscillating modes embedded in the signal. Two necessary conditions a constituent signal must satisfy to be termed as an IMF according to the definition are:

1) The number of zero crossings and the number of local extrema must either be equal to each other or differ by at most unity.
2) The mean of the upper envelopes defined by local maxima and that of lower envelopes defined by local minima should be zero.

3.1.1 Decomposition of Signal into IMF

The following steps should be followed for successful decomposition [50] of any signal into its constituent IMFs:

- ✓ First, identify all the local maxima points in the signal and then connect all the points with a cubic spline thus forming the upper envelope.
- ✓ Similarly, identify all the local minima points and repeat the procedure to form the lower envelope.
- ✓ Now the mean of the two (upper and lower) envelopes is taken and is represented as m_1 .
- ✓ Above steps are depicted in the image below.

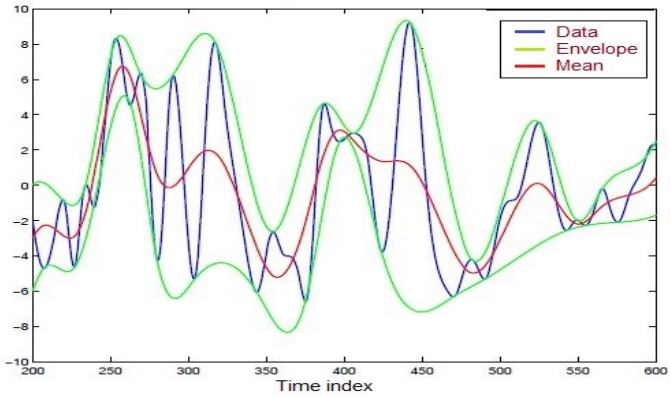

Fig 3.1. Decomposition step of EMD [52]

The thus obtained m_1 is now subtracted from the data to give the first component $h_1$as:

$$h_1 = x(t) - m_1 \tag{3.1}$$

This *sifting process* is needed to be iterated as many number of times as required so as the extracted signal reduces to IMF. In the subsequent sifting processes, $h_1$is regarded as a proto IMF and is considered as a new data for further processing; i.e.

$$h_{11} = h_1 - m_{11} \tag{3.2}$$

After performing this sifting process repeatedly, up to k number of times, h_{1k} finally takes the form of an IMF as:

$$h_{1k} = h_{1(k-1)} - m_{1k} \tag{3.3}$$

and is represented as: $c_1 = h_{1k}$, that is, the 1st IMF component obtained from the data.

A convergence test of Cauchy type is carried out to determine the stoppage criteria i.e. the value of k in equation (3.3). This test is a function of the two successive sifting outcomes defined as:

$$SD_k = \frac{\sum_{t=0}^{T} |h_{k-1}(t) - h_k(t)|^2}{\sum_{t=0}^{T} h^2{}_{k-1}} \tag{3.4}$$

If the value of the squared difference at kth level i.e. SD_k is less than that of a predefined threshold (typical value: 0.3) than further sifting is stopped and kth level IMF is obtained.

Residue $r_1(t)$ is obtained after subtracting the first IMF, i.e. $c_1(t)$ from the original signal as:

$$r_1(t) = x(t) - c_1(t) \tag{3.5}$$

The finest scale oscillation modes are represented by $c_1(t)$ while oscillations at longer time scales and other useful information is still embedded in $r_1(t)$. Hence, now residue signal is regarded as a new signal and repetitive sifting process is then applied onto it to obtain:

$$r_2(t) = r_1(t) - c_2(t)$$

$$r_3(t) = r_2(t) - c_3(t)$$

$$\cdot$$

$$r_n(t) = r_{n-1}(t) - c_n(t) \qquad (3.6)$$

The process is stopped when either

1) $r_n(t)$ becomes smaller than a predefined threshold, or
2) $r_n(t)$ becomes a monotonic or constant function.

Finally, the original signal can be written in terms of decomposed as a sum of the constituent 'n' IMFs and one residue:

$$x(t) = \sum_{i=1}^{n} c_i + r_n \ \ldots\ldots (3.7)$$

3.1.2 Advantages of EMD over Wavelet and Fourier Transforms

- Basis function for EMD is adaptively derived from the data while that for Wavelet and Fourier transforms, it is a priori.
- Feature extraction is not possible in Fourier, while for wavelets it is possible in continuous time domain only but is possible in EMD for both continuous and discrete time domain.
- Operation on Non-linear signal is possible only in EMD while it is not possible for Wavelets nor for Fourier Transforms.
- Operation on Non-stationary signals is possible both in EMD as well as Wavelets but is not possible in Fourier transforms.
- In EMD, the frequency is derived by differentiation while it is derived by convolution in case of Wavelets and Fourier transforms, hence it is not restricted by uncertainty principle unlike Fourier transforms which have global uncertainty and Wavelet transforms which have regional uncertainty.

3.1.3 Correction of Baseline drift noise using EMD

Empirical Mode Decomposition due to its characteristic nature has found plenty of applications in the denoising of ECG signals. The denoising in ECG signals using EMD has been mostly limited to EMG and Power line noises (high frequency noises) and very less attention has been given to baseline noise (low frequency noise). There are many works [28][29][30][31] in the literature which deals with the removing of high frequency noises by filtering the lower order IMFs but very few works has been proposed for correcting low frequency noise interference. Such works proposed by Na Pan *et al.* and Zhi-Dong Zhao *et al.* discusses about the baseline correction but comes with certain limitations as mentioned in the Literature review. The number of decomposition levels is a function of the variations (number of minima and maxima) in the original signal and the sampling frequency of the signal, thus the rigid approach of taking the last 'n' number of IMFs for the correction is not a robust way to deal with the problem.

We used EMD for denoising and tested its performance over different datasets constituting real time data as well as synthesised data but the results obtained were though good but not very satisfying. This is attributed to the fact that the baseline wander noise components are overlapping over different IMFs and are not limited to discrete IMF components. Therefore, if the BW noise components are tried to be completely removed, the information of the data is lost and if the information content is tried to be preserved, than the noise components also remains. Another major challenge with the described algorithms is to decide on the number of IMFs which are corrupted by the baseline noise components. Thus a criterion has been set which selects the minimum number of IMFs which do not contains any valuable information content.

In the figure below, the decomposition of an ECG signal superimposed with low frequency baseline noise is illustrated. The noisy ECG signal when decomposed, breaks down into 14 unique IMFs and one residue. The frequency spectrum of each IMF is plotted against each decomposed signal. As can be observed from the graphs, the lower order IMFs constitutes the finest scale variations (high frequency) of the original signal while higher order IMFs constitutes the low frequency variations and thus contains the baseline noise components present in the original signal. Therefore, to filter out baseline noise using EMD these higher order IMFs containing low frequency noise components are discarded and the rest of the IMFs are reconstructed to give back the filtered signal.

1st IMF

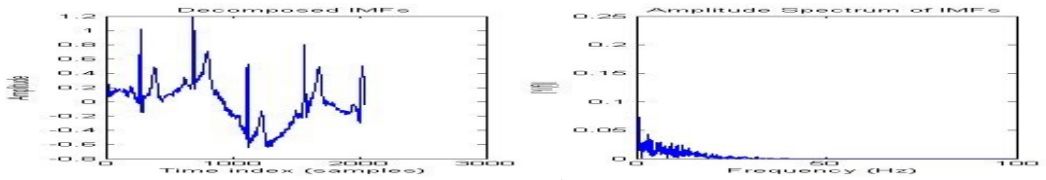

2nd IMF

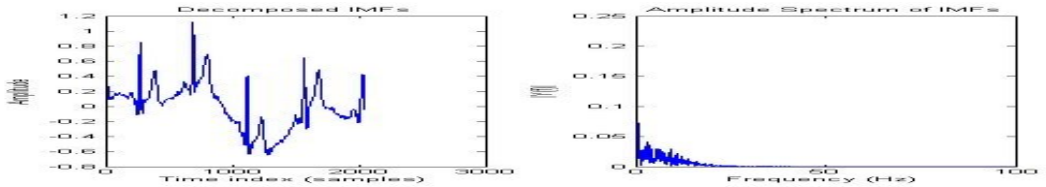

3rd IMF

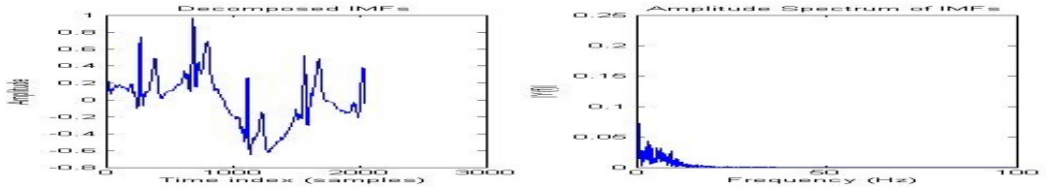

4th IMF

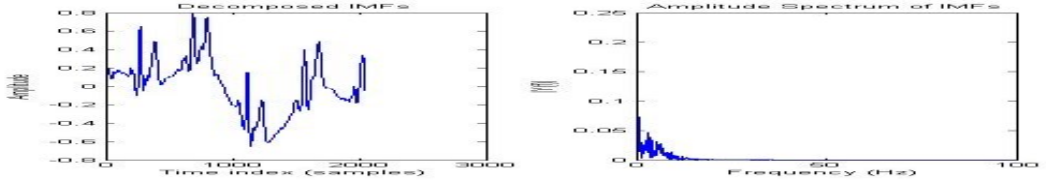

5th IMF

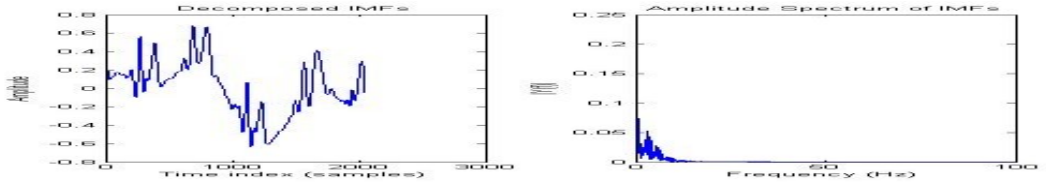

6th IMF

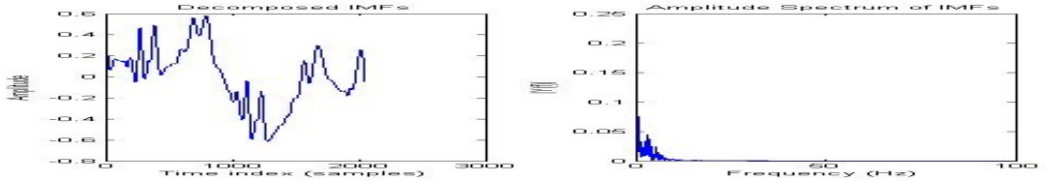

7th IMF

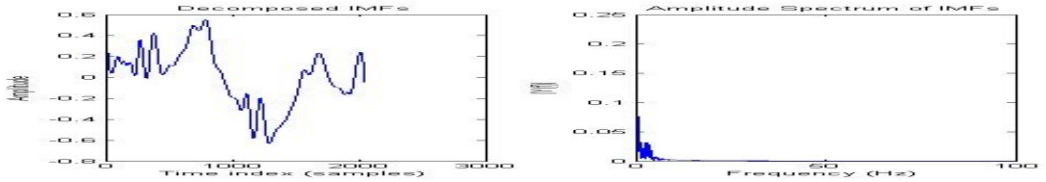

8th IMF

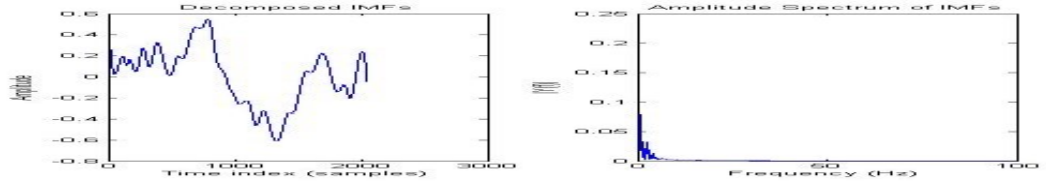

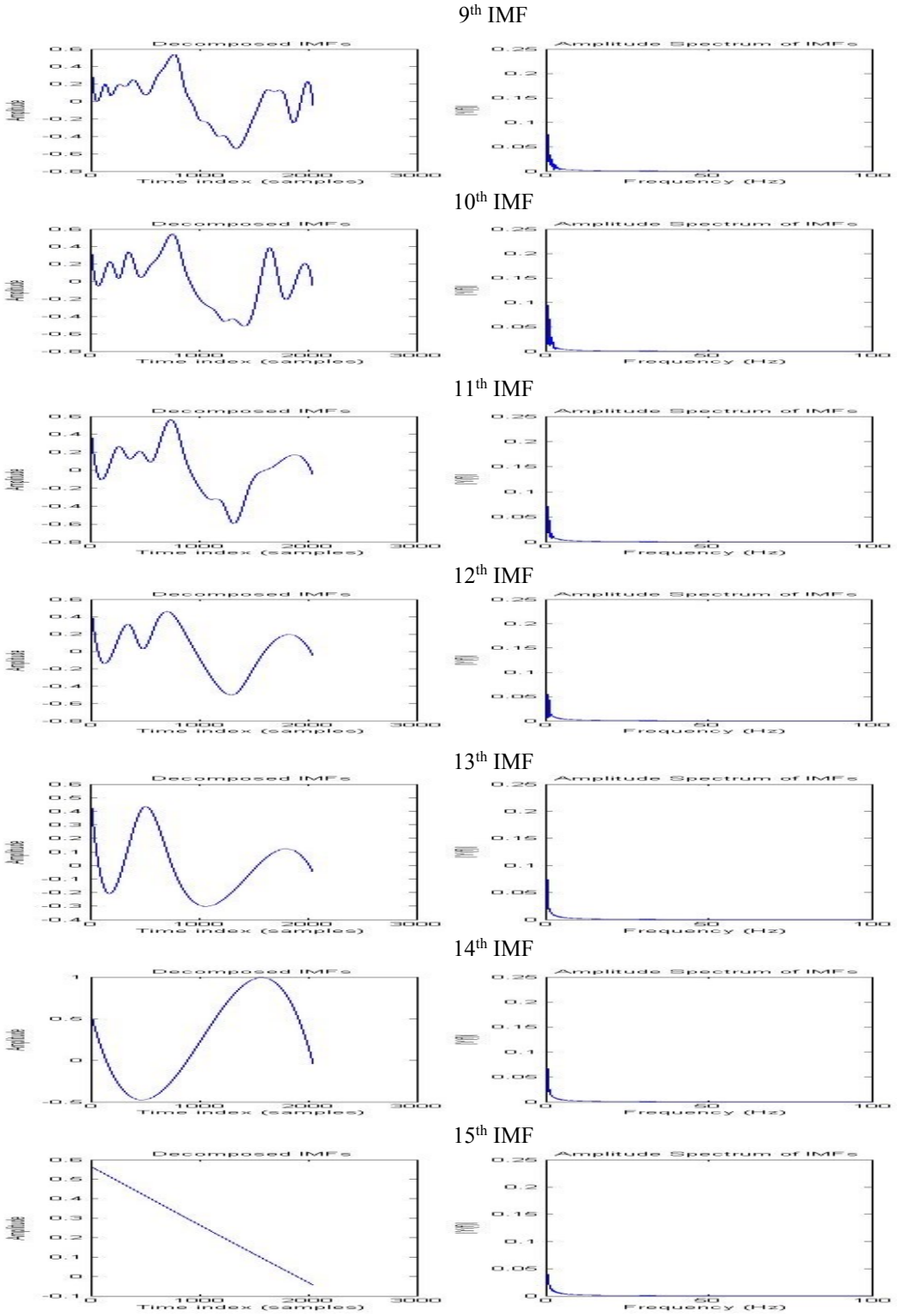

Figure 3.2: Decomposition of Baseline noise corrupted real ECG signal (person1 - rec7) into constituent IMFs along with the frequency spectrum of each IMF.

3.2 Morphological Filters

The discipline of mathematical morphology was introduced for the first time by G. Matheron and J. Serra on the basis of geometry. In the recent past, Mathematical Morphology has gained considerable attention and has emerged as a strong tool for signal processing. Initially the morphological filters find applications in image (2-D signals) processing [53]. The morphological filters have now also been extended to 1-D signals. The concept of 1-D morphology in the field of ECG was first time exploited by P. E. Trahanias [51] in his work, "An approach to QRS complex detection using mathematical morphology". Many algorithms have been developed since then around the morphological filters for ECG denoising.

3.2.1 Basics of Morphological Operations

Mathematical morphology is a discipline of mathematics which is an efficient non-linear signal processing tool capable of retaining the shape information content of the signal. Structuring element or 'SE' is the most fundamental element of morphological filters. The geometry of these structuring element forms a very important role in determining the nature of the morphological filter. The shape information content of a signal can be extracted by varying the shape (a point, a line, a circle etc.) and size of the structuring element. Varied results are obtained by varying the geometry of a SE.

The two most basic morphological operations [53] available are:

1) Erosion, and
2) Dilation

For a one dimensional signal such as ECG erosion and dilation operations are defined as follows. Let $f(n)$, be the input to the morphological filter with structuring element as $l(m)$, where $n = (0,1,2 \dots, N-1)$ and $m = (0,1,2, \dots, M-1)$ while $N \gg M$, then mathematically;

Erosion is given as: $$(f \Theta l)(n) = \min_{m = 0,..M-1} \{f(n+m) - l(m)\} \quad (3.8)$$

while, $n = (0,1, \dots, N-M)$ and,

Dilation is given as: $$(f \oplus l)(n) = \max_{m = 0,...M-1} \{f(n-m) + l(m)\} \quad (3.9)$$

while, $n = (0,1, \dots, N-M)$.

Erosion operation when applied on two dimensional images is used for disjoining of two separate objects joined under the influence of noise. In the same manner, dilation operation fills the pits (holes) emerged in a noisy image.

Two another very important signals derived from erosion and dilation operations are opening and closing operations defined as follows:

$$\text{Opening: } (f \circ l)(n) = (f \ominus l \oplus l)(n) \tag{3.10}$$

$$\text{Closing: } (f \bullet l)(n) = (f \oplus l \ominus l)(n) \tag{3.11}$$

Opening operation is defined as erosion followed by dilation and is responsible for eliminating the peaks and smoothening the contour. Closing operation is defined as dilation followed by erosion and is responsible for eliminating pits, small gaps and discontinuities.

The major advantage in using morphological filtering for noise removal in ECG signals is that the transform is a function of the morphology, shape of the input and is independent and uncorrelated to the frequency of the signal. Hence the morphology of the input signal is preserved which is an important consideration for denoising of ECG signals as the morphology of an ECG signal holds critical information of the state of heart.

3.2.2 Designing of morphological filters for Baseline Wander removal

The peak and pits of a signal can be removed by combining the two opening and closing operations together. This concept is utilised for removing the present morphologies (i.e. QRS complex, P and T waves) in an ECG signal. These morphologies are removed first from the original baseline noise corrupted signal so that the baseline noise can be estimated. This estimated baseline noise is then subtracted from the original signal to eliminate the baseline noise. To remove the morphologies present in the ECG signal, the size of the structuring element is needed to be set in proportion to that of the part to be extracted. This can be further understood as supposedly, QRS complex has to be extracted using morphological filter than the length of the SE must be slightly greater than that of the QRS complex. If ‘S1’ is the length of the SE, then if;

- S1 > length of variation: variation is removed, and if;
- S1 < length of variation: variation is retained.

In this way, removing all the morphologies present in the ECG we would be left with only the longer variations (low frequency baseline noise) and hence proper baseline can be estimated.

In order to extract the morphologies in the cardio signal more evenly and prevent one-way migration the opening and closing operations are merged (given by Margos [54]) together in both the possible orders and then the average is taken for both the combinations. The opening and closing functions are cascaded as following:

$$OC\big(f(n)\big) = (f \circ l \bullet l)(n) \tag{3.12}$$

$$CO\big(f(n)\big) = (f \bullet l \circ l)(n) \tag{3.13}$$

The filters described in equations (3.12) and (3.13) are taken together and averaging is performed as:

$$OC - CO = \frac{OC\big(f(n)\big)+CO\big(f(n)\big)}{2} \tag{3.14}$$

The model of the morphological filter used in this work is depicted in the block diagram:

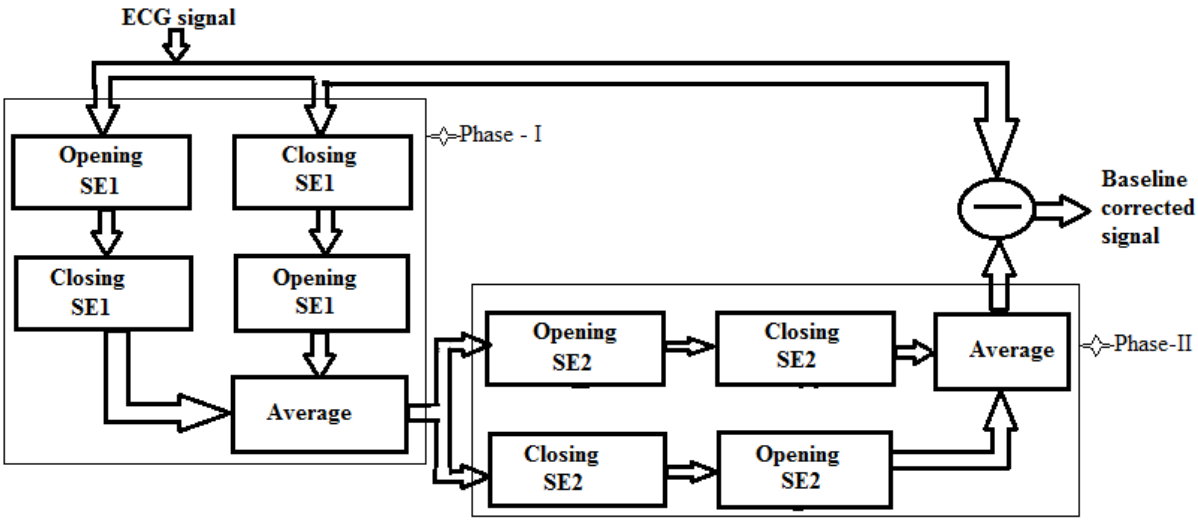

Fig.3.3 Block diagram representation of morphological filter design

As seen from the block diagram, the ECG signal is initially fed to phase-I of the filtering operation. The phase-I is responsible for extracting the QRS complex from the ECG signal. The output of phase-I is given as input to the phase-II of morphological filters. Phase-II is responsible for removing the P and T waves present in the signal. Once these morphologies are extracted from the signal, the baseline of the signal can be approximated. This approximated baseline is then subtracted from the noisy signal to

obtain baseline corrected ECG signal. The extraction of the morphologies of the cardio signals is carried out in two separate steps as in [35][36][37] because if all the morphologies of varied lengths present in signal are tried to be removed at once, the signal information may be lost and severe distortion in the actual baseline may appear in the output. The duration of different morphologies are listed in the table below:

Table 3.1 Time duration of characteristic waves in ECG

Characteristic Wave	duration in seconds
QRS complex	0.06 ~ 0.10s
P wave	0.08 ~ 0.11s
T wave	0.05 ~ 0.25s

As observed from the table, T wave is the longest wave present in the ECG signal while QRS complex has the shortest duration. The length of the structuring element has to be a function of these duration of characteristics waves. To extract any particular wave, the length of the structuring element must be greater than that of the duration of the wave. The QRS complex has highest amplitude and hence it is extracted out separately first and then the remaining two waves are removed.

The structuring element as in [37] for phase-I designated as 'SE1' is chosen in a way such that the length of 'SE1' is greater than the number of samples consumed in QRS complex, i.e.: *SE1 > number of samples of QRS complex;*

While; *number of samples = PW * Fs;* PW: pulse width and Fs: sampling frequency of signal.

In a similar manner, 'SE2' for phase-II of the morphological filter is chosen to be greater than the number of samples consumed by the longest wave i.e. the T wave. In this way, all the waves present in the cardio signal are extracted.

The major challenge encountered in deciding on the length of the structuring element for phase-II, i.e. SE2 is that, the duration of these characteristic waves are not fixed. There are variations observed in the duration of the characteristic waves in:

- ECG of one subject to other: duration of QRS complex, R-R interval, P and T wave all varies in the average band from one subject to another.

- At higher heart rate: the R-R interval and thus QT and ST segment length reduces as the heart rate increases (as in case of exercise ECGs [38]). Also, an upward slope is observed in the ST segment as the heart rate increases considerably.
- Within ECG of a single Subject: there may be slight variations in the lengths arising within the ECG of a same subject at different times.
- In case of any arrhythmia: the duration of the important segments are altered in case the subject is suffering from any particular arrhythmia. For instance: in case of atrial fibrillation, the R-R interval continuously varies.
- In infants and new-borns: the waves duration are different for infants.

To tackle this problem in morphological filtering, some adaptive and data driven mechanism must be adopted. This challenge is taken up in this work and a data driven structuring element is suggested which makes the structuring element partially adaptive to the variations in ECG morphology. The duration of QRS complex sees much less variations as compared to other characteristics waves. Hence, the length of the structuring element for phase-I of the morphological filters is left unaltered and is taken as a measure of the defined biological duration of the QRS complex. However, the length of the structuring element 'SE2' defined for phase-II is made adaptive and is derived from the data. The details has been discussed in the following sections.

3.3 QRS Detection

QRS complex in an ECG signal is the most salient and visible feature of the electrocardiogram. The QRS complex is a representation of the electrical activities that takes place in the heart during ventricular contraction. The shape as well as the time interval of its occurrence reveals a lot of information important for effective medical diagnosis of the signal. Because of its noticeable and distinct shape this characteristic wave is used as a reference for calculations of the heart beat and other details. Hence, QRS complex detection is a fundamental step for most of the automated ECG signal processing algorithms.

Many algorithms have been developed till date which deals with the problem of accurate detection of the QRS pulse. Here we are using very basic derivative based approach given by Pan and Tompkins [55] which exploits the characteristic slope of QRS complex for successful detection of the pulse. Though many advanced algorithms have been developed lately, but this basic approach is used in this algorithm for the reasons stated

below:

1) The baseline noise components have already been suppressed by EMD and the signal is pre filtered for other high frequency noises while the said algorithm by Pan and Tompkins, is proven to give good results when noise content in the signal is minimal. Hence, very high degree of accuracy is achieved.
2) This algorithm is computationally inexpensive and is very easy to implement compared to other similar algorithms.
3) Still if any erroneous R peak is detected, we are interested only in the average R-R length and the erroneous R-R length is removed and is not included in the averaging process.

Thus, without any alter effect this basic algorithm for QRS detection by Pan and Tompkins is utilised effectively in this algorithm, making the novel approach computationally efficient.

3.3.1 QRS detection algorithm model

The algorithm used for QRS detection is typically based on the characteristic slope of the QRS pulse. The QRS complex has the steepest and thus the maximum slope among all the variations present in the ECG signal. Thus taking the derivative of the ECG signal we can exploit this property for detecting the peaks of the QRS complex. This can be understood from the block diagram as under:

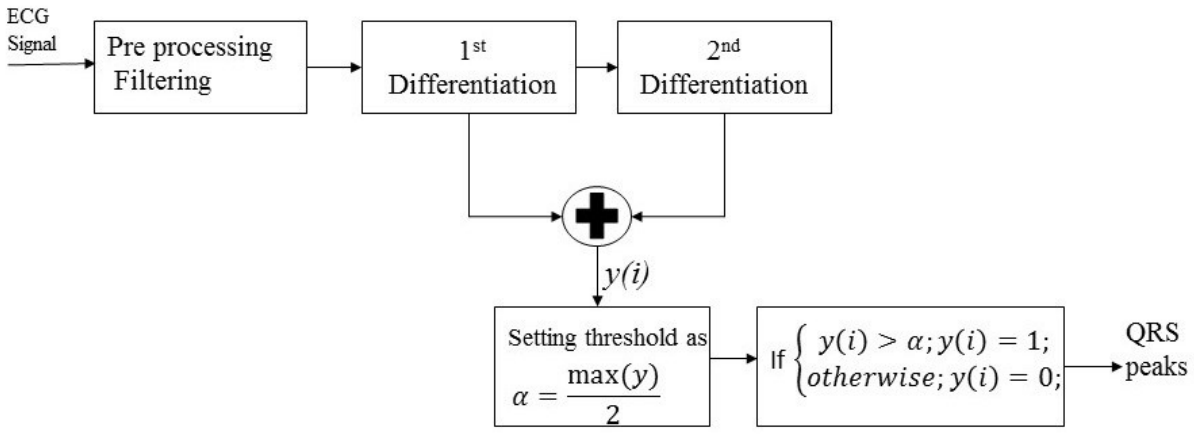

Fig. 3.4: QRS detection-basic block description

In the algorithm, two times derivative of the input signal has been taken so that the noises and false indicative slopes can be eliminated. The threshold has been selected as half of

the maximum value of the cumulative differentiation signal. This threshold has been validated with simulations on different signals and is found to give good results. The threshold is good enough to suppress all the unwanted details and retains only the peak of the QRS complexes. Thus at the end of it we get the locations of the QRS complexes.

The graph in support to the above block diagram are presented in figure 3.5. In the graph, the graph at the top is the filtered ECG. First and second time differentiated signals are added to give the cumulative signal. The threshold is estimated from this signal. The graph at the bottom depicts the detected QRS complex which is detected very precisely at the correct locations.

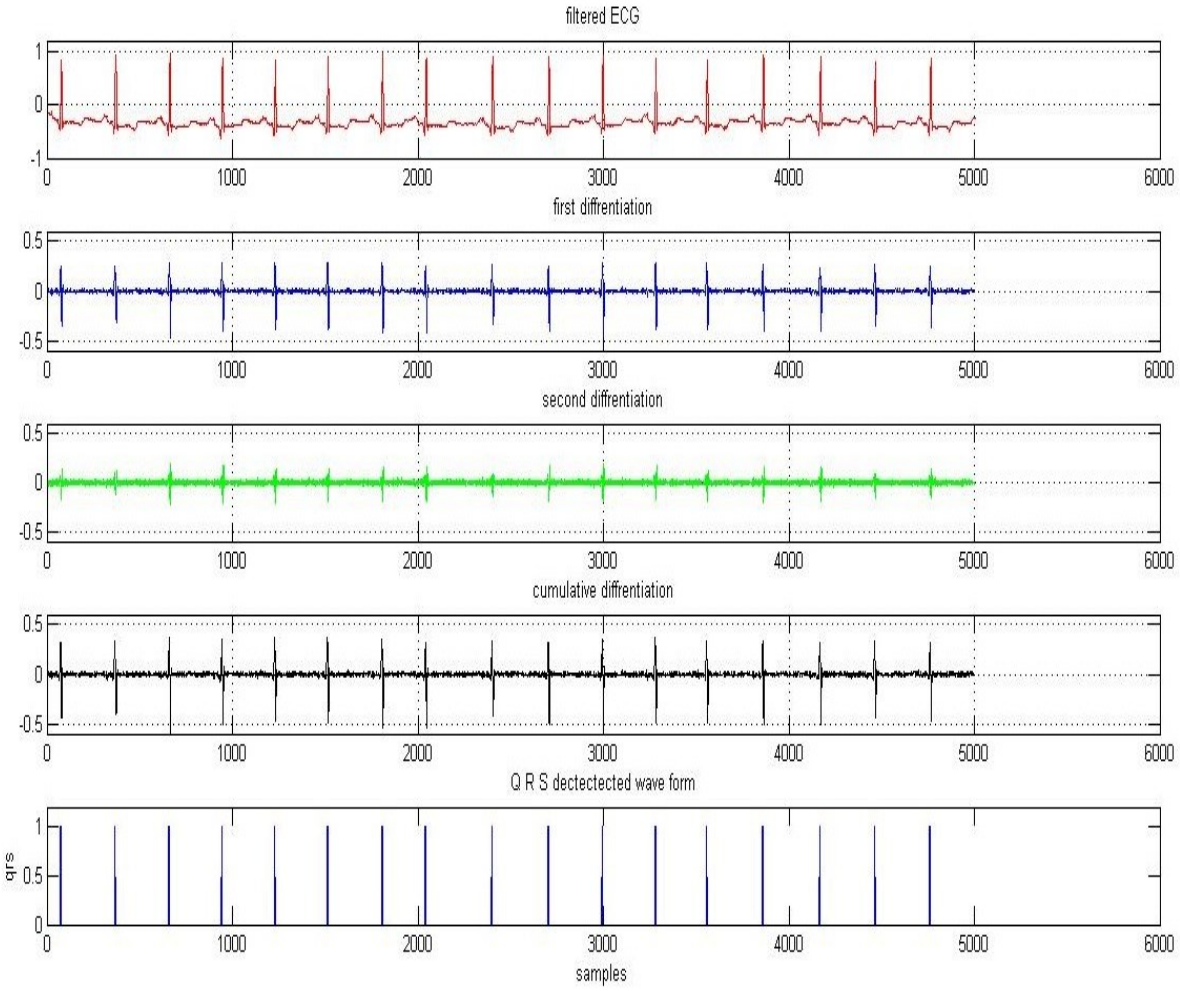

Figure 3.5: Graph for QRS complex detection.

3.4 Proposed Algorithm

The overall algorithm can be understood from the flow diagram drawn below. The steps followed in the algorithm are listed below assuming $x(n)$ is the input baseline corrupted ECG:

First, the signal is breakdown into its constituent IMFs using empirical mode decomposition. $$x(n) = \sum_{i=1}^{N} c_i(n), \quad (3.15)$$

Where, *N* denotes the number of IMFs the signal *x(n)* is decomposed to, and $c_i(n)$ represents the i^{th} intrinsic mode, while the residue is assumed to be the last IMF.

Secondly, for identifying 'm' baseline corrupted noisy IMFs, m is calculated as:

$$m = round(0.24 * N) \quad (3.16)$$

N has been multiplied by a factor of *0.24*. This factor is chosen on the experimental basis by simulating multiple times with different values of *scaling factor*. So that the new reconstructed signal with baseline correction is given as:

$$\hat{x}_{emd}(n) = \sum_{i=1}^{N-m} c_i(n) \quad (3.17)$$

Now this reconstructed signal $\hat{x}_{emd}(n)$, with the help of empirical mode decomposition has been partially denoised by the empirical mode decomposition and is termed as approximate denoised ECG. This denoising is partially completed because the baseline noise is overlapping over a number of intrinsic modes. So, if more number of IMFs are eliminated the information content suffers. Hence, minimum number of IMFs are removed which contains most of the noise.

Next, this baseline corrected signal is given as input to morphological filter (phase-I) with structuring element length given as:

$$SE1 = 0.11 \times Fs \quad (3.18)$$

here, Fs is the sampling frequency of the input signal and the value '0.11' has been taken as indicated in Table 3.1. This is the width of the QRS pulse known from medical terms and it hardly varies until in the case of serious cardiac abnormalities. There are many shapes possible for a structuring element for example: linear, circular, point etc., but for one dimensional ECG signal linear shape was found to give consistently good results, hence a linear structuring element has been used in this work.

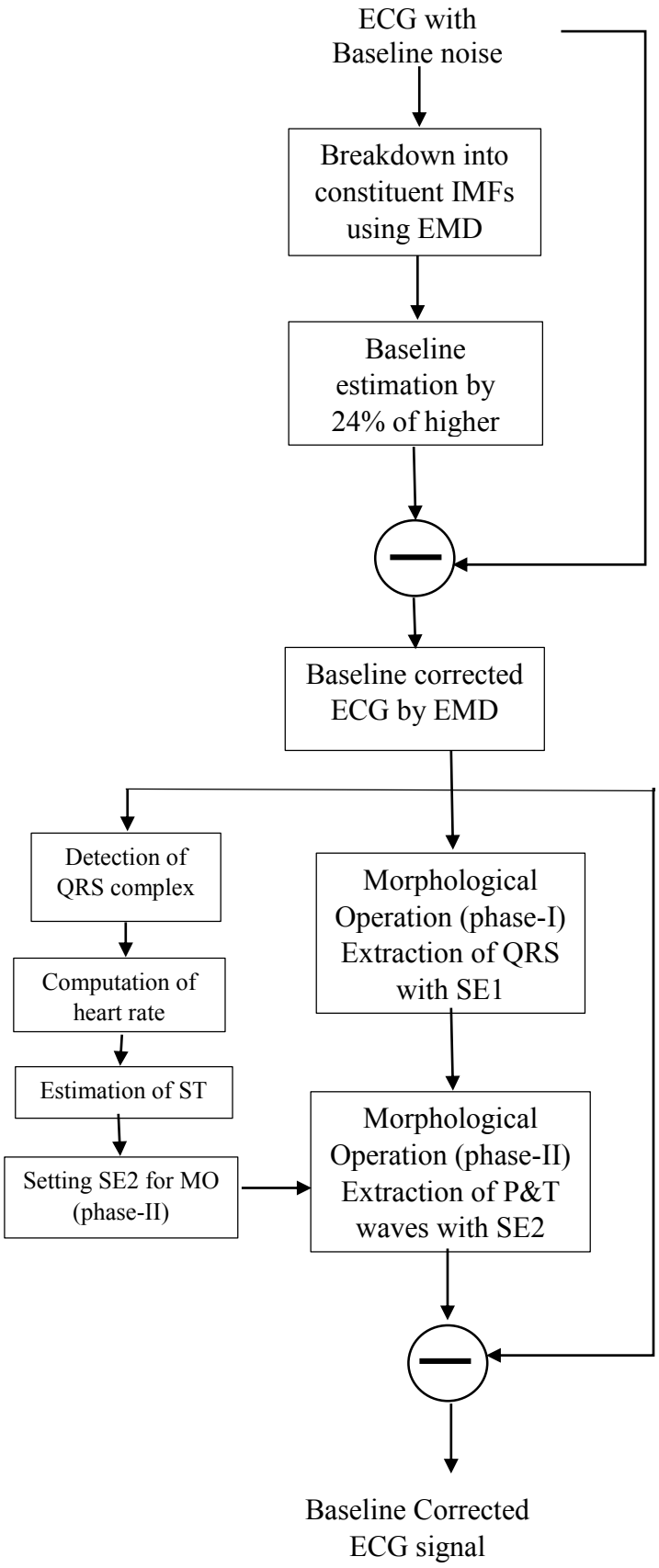

Fig. 3.6: Detailed block level Description of complete Algorithm

So, morphological filtering is performed over the corrected ECG with a linear structuring element say l_1 of length *SE1* and with the origin kept at the centre then,

$$\hat{x}_{mp1}(n) = \frac{(\hat{x}_{emd} \circ l_1 \bullet l_1)(n) + (\hat{x}_{emd} \bullet l_1 \circ l_1)(n)}{2} \tag{3.19}$$

$\hat{x}_{mp1}(n)$ denotes the output of the morphological filters (phase-I), i.e. QRS extracted pulse from ECG signal previously denoised by the empirical mode decomposition.

The same baseline corrected signal produced by EMD, i.e. $\hat{x}_{emd}(n)$ is also given to the QRS detection algorithm designed for detection of R peaks. First, the differentiation step is performed as, first differentiation:

$$\dot{g}(n) = \frac{d\hat{x}_{emd}(n)}{dn} \tag{3.20}$$

second differentiation:

$$\ddot{g}(n) = \frac{d\hat{x}_{emd}(n)}{dn} \tag{3.21}$$

cumulative differentiation:

$$y(n) = \dot{g}(n) + \ddot{g}(n) \tag{3.22}$$

threshold (β) selection:

$$\beta = \frac{max(abs(y(n)))}{2} \tag{3.23}$$

with β as the threshold, the signal containing peaks is described as:

$$y_{R-R}(n) = \begin{cases} 1\,; & if\ y(i) > \beta \\ 0; & if\ y(i) < \beta \end{cases} \tag{3.24}$$

while $i = 0,1,....,L$ and L is the number of samples in the signal.

With the help of this $y_{R-R}(n)$ signal, the average distance between the two R-R peaks is calculated and is denoted by *avg_R-R*. This data derived value of RR peak distance is then used for estimation of the heart rate.

As clear from the Table 3.1, characteristic wave T is of longer duration than the S wave. Therefore, conventionally the length of T is been used for morphological operation (phase-II) as in [37], but this value of T varies to a large extent under various

circumstances and is not a constant. Thus, a data driven approach is adopted to set the value for *'SE2'*. In this research work, ST interval has been used for setting the length of the structuring element for phase-II morphological filtering.

There are various advantages associated with this modified length of SE. Under normal circumstances, ST interval is larger than the T wave duration. Thus both the P and T waves can easily be extracted using the ST interval as the structuring element for phase-II of morphological filters. Another, very important factor that complements our decision of taking ST interval as the length for 'SE2' is that, as the heart rate increases, there has been an upward slope noticed in the ST segment. This finding is more popular in exercise ECGs. An excerpt from the book titled, "Practical ECG for Exercise Science and Sports Medicine" by Greg Whyte [56] is given in Appendix-II.

This study reflects the important cardiac changes being recorded at the time when the heart rate is high. The important points that can be exploited for determining the length of structuring element are:

1. QT interval shortens as the heart rate increases.
2. An upward slope in ST interval as heart rate increases.
3. Minimal shortening of QRS complex.

Thus as the heart rate increases the upward slope induces much more baseline drift in the signal. Hence, taking ST interval as the length for structuring element also eliminates the induced slope in the ST interval due to high heart rate. Also as the heart rate increases, the ST interval experiences a heart rate related shortening. So, overall effect of taking ST interval as the length for structuring element makes the algorithm adaptive to the heart rate variations in the ECG signal.

So, now a linear structuring element of length SE2 equivalent to the ST interval with its origin at center is constructed say, l_2 then the output of morphological filter phase-I. i.e. $\hat{x}_{mp1}(n)$ is given as the input to the morphological filter phase-II to give the final estimated baseline in approximated denoised ECG as $\hat{x}_{mp2}(n)$:

$$\hat{x}_{mp2}(n) = \frac{\left(\hat{x}_{mp1} \circ l_2 \bullet l_2\right)(n) + \left(\hat{x}_{mp1} \bullet l_2 \circ l_2\right)(n)}{2} \tag{3.25}$$

The eq. (3.25) represents the estimated baseline in the approximated denoised ECG signal. This baseline is then subtracted from the approximated ECG signal to give the finally denoised ECG signal given as:

$$\hat{x}_{denoised}(n) = \hat{x}_{emd}(n) - \hat{x}_{mp2}(n) \tag{3.26}$$

So, finally equation (3.26) gives the denoised ECG signal using the proposed algorithm.

Chapter 4

RESULTS AND DISCUSSIONS

In this chapter, the results after simulation have been compiled. This chapter is organized in the following manner. In the first section, the ECG Database used are described in detail, subsequent section describes the methods for quantification of results followed by a discussion on generated noises. Further sections shows the results for a simulated ECG, in followed by denoising results over the real ECG signal are presented.

4.1 ECG Signal Database

Several different signals have been tested against the algorithm to check the robustness and validity of the results. Built in simulated ECG available in MATLAB R2011b was used to derive the results for the simulated ECG. 512 samples per cycle is taken to construct the ECG signal. The ECG signal is then smoothed by a ninth order Savitzky-Golay filter. The signal thus obtained is repeated eight times so that a natural looking ECG signal is obtained making the total number of samples count as 4096. One such sample signal is shown in the figure below:

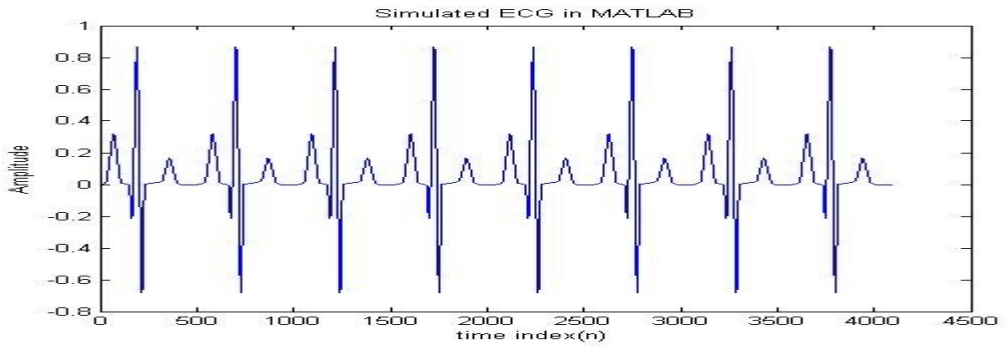

Fig 4.1: Simulated ECG in MATLAB

Original ECG signals obtained from different subjects has also been taken up to test the algorithm for real ECG. A lot of signals were used while execution and compilation of results to test the adaptive nature of the proposed algorithm. The algorithm has been made robust against variations in the heart rate and hence signals with different heart rates are taken up to validate our results.

PhysioBank [57] is an emerging archive of well-characterized recordings in digital form of physiologic signals and the associated data for the use of community for biomedical research. It incorporates databases of multi-parameter neural, cardiopulmonary and other medical signals from healthy subjects and from patients with diverse conditions suffering from major public health implications, including congestive heart failure, sudden cardiac death, gait disorders, epilepsy, aging and sleep apnea.

The ECG-ID Database [58]: It consists of 310 ECG recordings, obtained from 90 persons. Each recording comprises of 20 seconds of recorded lead I of ECGs, sampled at 500 Hz with 12-bit resolution for a range of ±10 mV;

The obtained records are from volunteers out of which 46 were women and 44 were men whose age varies from 13 to 75 years. The total number of recordings taken for a single subject varies from 2 (collected in a day) to 20 (collected periodically over 6 months).

The obtained raw ECG signals were noisy and contains both high frequency and low frequency components of noise. Each of the compiled record comprises of both raw ECG and filtered ECG signals:

- Signal 0: ECG I (raw signal)
- Signal 1: ECG I filtered (filtered signal)

4.2 Quantification of Results

To quantify the performance of our proposed algorithm compared to other algorithms, the performance is evaluated with Mean Square Error (MSE), Signal to Noise Ratio (SNR) and cross-correlation coefficient (ρ_{x-dn}). Mathematically, mean square error is given as:

$$MSE = \frac{1}{N}\sum_{i=1}^{N}(x(i) - dn(i))^2, \tag{4.1}$$

Signal to Noise ratio (SNR) of the input (noisy) ECG and SNR of output (denoised) ECG:

$$SNR_{input} = 10\log_{10}\left[\frac{\sum_{i=1}^{N} x(i)^2}{\sum_{i=1}^{N}(x(i) - n(i))^2}\right] \tag{4.2}$$

$$SNR_{output} = 10\log_{10}\left[\frac{\sum_{i=1}^{N} x(i)^2}{\sum_{i=1}^{N}(x(i)-dn(i))^2}\right] \tag{4.3}$$

And, the cross-correlation is given as:

$$\rho_{x-dn} = \frac{\sum_{i=0}^{N} x(i)dn(i)}{[\sum_{i=0}^{N} x^2(i)\sum_{i=0}^{N} dn^2(i)]^{1/2}} \tag{4.4}$$

where, *x(i)* is the pure ECG signal, *n(i)* is noisy ECG, *dn(i)* is denoised ECG and *N* is the total number of samples.

4.3 Generation of Different Low Frequency Noise

The results for simulated ECG signal are compiled by first adding low frequency noise to the signal and then denoising it using the proposed algorithm. The same noisy signal is also denoised using wavelets, EMD technique and morphological filters. The final results are tabulated for an easy view. To check the robustness of the algorithm, different noises of varied amplitude, frequency and SNR are added to the pure simulated ECG.

Mathematically, the six noises that has been added are described below:

Noise 1: two sine waves of frequency 0.2 Hz and 0.45 Hz of amplitude 0.33 and 0.22V respectively with SNR (noisy) = -3.1043 and MSE (noisy) = 0.0781.

Noise 2: two sine waves of frequency 0.15 Hz and 0.45 Hz of amplitude 0.22 and 0.33V respectively with SNR (noisy) = -2.7397 and MSE (noisy) = 0.0718.

Noise 3: two sine waves of frequency 0.25 Hz and 0.50 Hz of amplitude 0.22 and 0.3V respectively with SNR (noisy) = -2.5784 and MSE (noisy) = 0.0692.

Noise 4: two sine waves of frequency 0.25 Hz and 0.60 Hz of amplitude 0.33 and 0.22V respectively with SNR (noisy) = -3.0277 and MSE (noisy) = 0.0767.

Noise 5: two sine waves of frequency 0.40 Hz and 0.60 Hz of amplitude 0.33 and 0.22V respectively with SNR (noisy) = -2.2758 and MSE (noisy) = 0.0645.

Noise 6: triangular wave of frequency 0.20Hz of amplitude 0.1V and sine wave of frequency 0.15Hz of amplitude 0.22V with SNR (noisy) = 2.2903 and MSE (noisy) = 0.0226.

While generating these noises, the maximum frequency of the noisy additive waves has always been kept below 0.6Hz, as baseline noise exists below this frequency band only. The noises are shown graphically below:

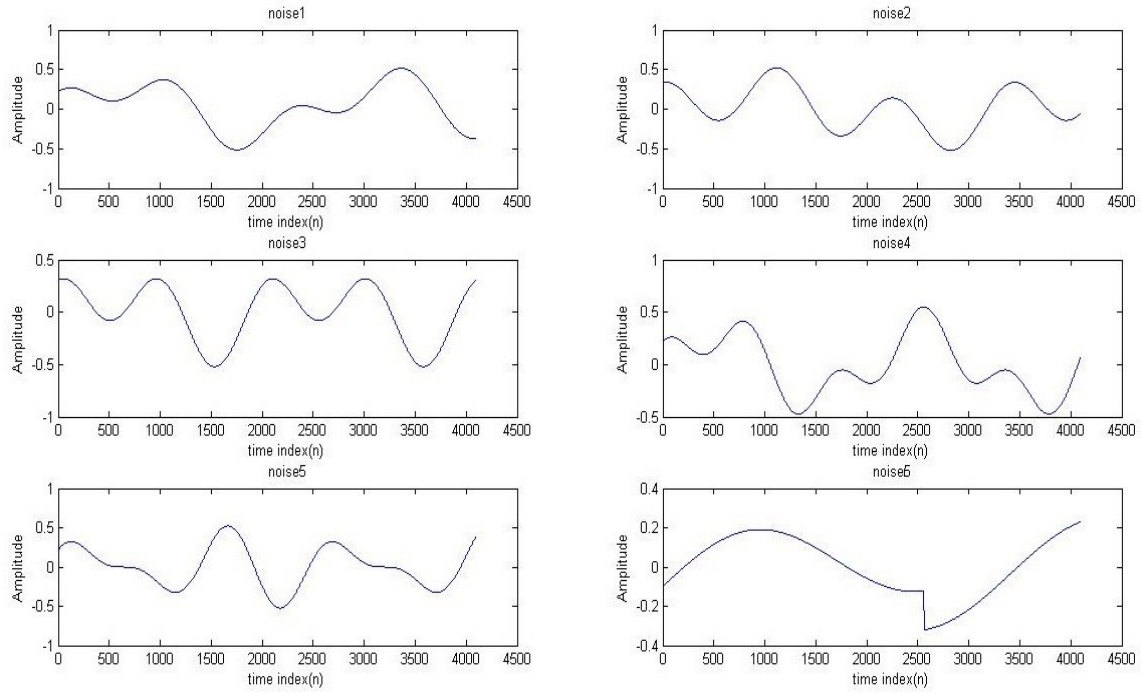

Fig 4.2: Six different noises with varied frequency and amplitude added to ECG.

4.4 Simulation Results for Simulated ECG

The simulation results for the simulated ECG signal corrupted with different noises are compiled below in graphical and tabular form. Following graphs presents the algorithm in a step by step form, and finally the obtained result for a pure ECG signal corrupted with *Noise 2* (as discussed above).

In figure 4.3, the *first graph* shows the pure simulated ECG signal used for simulation. This ECG signal is pre-processed by using Savitzky-Golay filter. The ECG signal is then added with *Noise 2* (as above), to give the noisy ECG as is shown in *graph 2*. Then, the noisy signal is decomposed into its constituent intrinsic modes. The signal decomposes into 10 IMFs. According to our set criterion, last 24% of the IMFs i.e. the last 3 (rounded off) IMFs are used to estimate the baseline noise from the signal as depicted in *graph 3*. This estimated baseline noise is then subtracted from the noisy signal to obtain baseline corrected ECG signal as shown in *graph 4*. Now, using this approximate baseline

corrected signal, QRS complex are detected as presented in *graph 6*. *Graph 5*, shows QRS extracted ECG signal. This QRS extracted signal is obtained from the approximated baseline corrected signal after passing it through morphological filters (phase-I). Next, the length of structuring element for morphological filters (phase-II) is selected as the approximated length of ST segment. So now, the QRS extracted signal is passed through the morphological filters (phase-II) to extract the remaining morphologies of the ECG signal. The left over signal represents the baseline variations present in the approximated baseline corrected ECG signal and is depicted in *graph 7*. These minute variations in the baseline are further subtracted from the approximated signal to give the final denoised ECG signal as in *graph 8*.

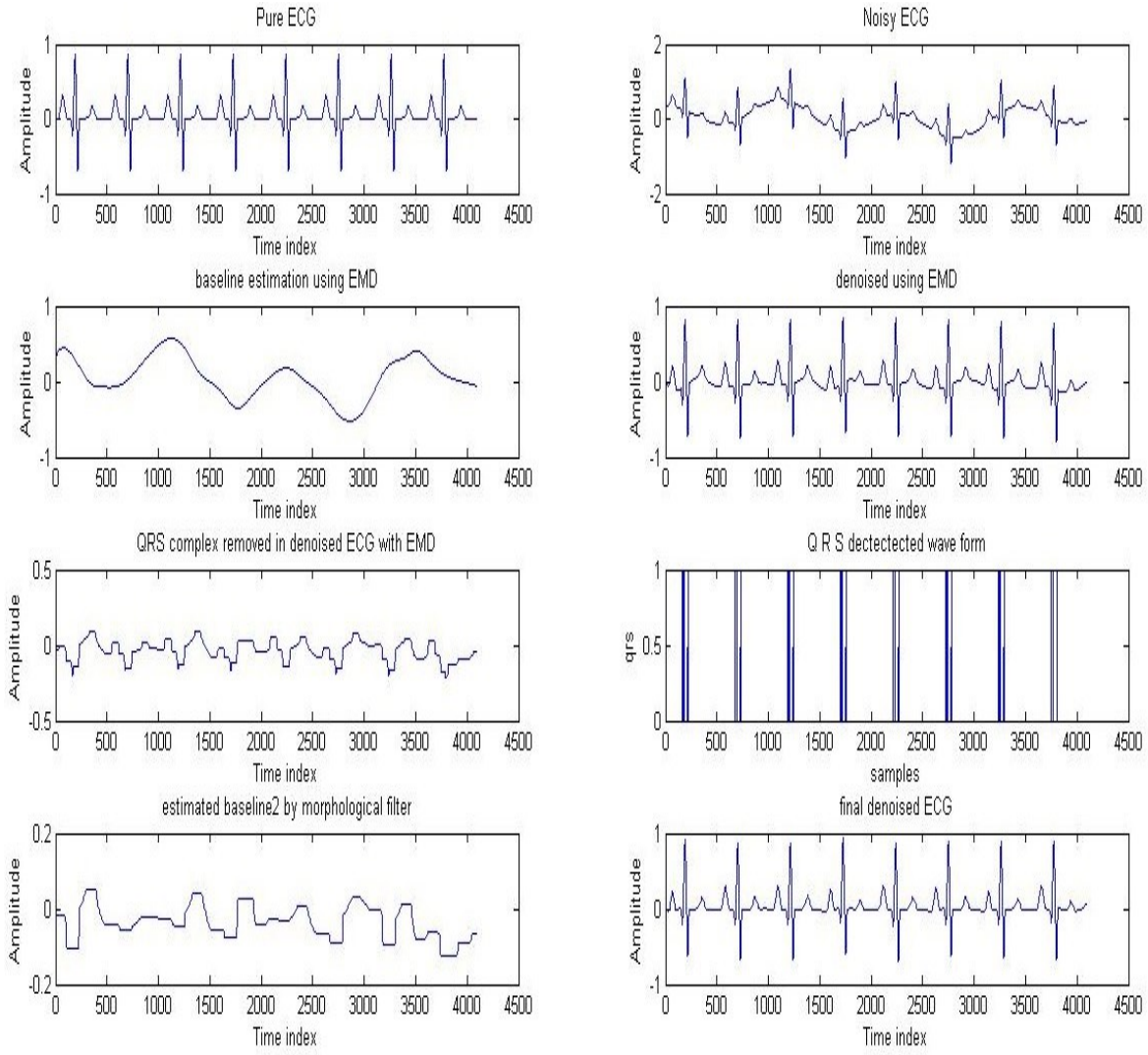

Fig 4.3: Results for simulated ECG: corrupted with *Noise 2*

The tabulated results are shown below, which compares the effectiveness of the proposed algorithm as compared to Wavelets, only EMD and only morphological operators against all the six different noises discussed above.

Table 4.1: Results for Simulated ECG with *Noise 1*
SNR (input) = -3.1043; MSE(noisy) = 0.0781

	Using Wavelet		Only EMD	Only Morphological	Our Algorithm
	HT	ST			
MSE	0.0034	0.0221	0.0064	0.0017	0.00084
SNR	10.5173	2.3821	7.7912	13.6166	16.5641
Cross-correlation	0.9554	0.7987	0.9167	0.9783	0.9890

Table 4.2: Results for Simulated ECG with *Noise 2*
SNR (input) = -2.7397; MSE(noisy) = 0.0718

	Using Wavelet		Only EMD	Only Morphological	Our Algorithm
	HT	ST			
MSE	0.0068	0.0215	0.0041	0.0023	***0.00075***
SNR	7.5284	2.5070	9.6869	12.1739	***17.0676***
Cross-correlation	0.9124	0.7991	0.9453	0.9693	***0.9903***

Table 4.3: Results for Simulated ECG with *Noise 3*
SNR (input) = -2.5784; MSE(noisy) = 0.0692

	Using Wavelet		Only EMD	Only Morphological	Our Algorithm
	HT	ST			
MSE	0.0129	0.0158	0.0061	0.0023	***0.0009***
SNR	4.7008	3.8326	7.9603	12.1253	***16.2568***
Cross-correlation	0.8490	0.8280	0.9191	0.9691	***0.9882***

Table 4.4: Results for Simulated ECG with *Noise 4*
SNR (input) = -3.0277; MSE(noisy) = 0.0767

	Using Wavelet		Only EMD	Only Morphological	Our Algorithm
	HT	ST			
MSE	0.0133	0.0197	0.0041	0.0021	***0.0012***
SNR	4.5774	2.8849	9.6869	12.5007	***15.1385***
Cross-correlation	0.8433	0.8047	0.9453	0.9718	***0.9846***

Table 4.5: Results for Simulated ECG with *Noise 5*
SNR (input) = -2.2758; MSE(noisy) = 0.0645

	Using Wavelet		Only EMD	Only Morphological	Our Algorithm
	HT	ST			
MSE	0.0252	0.0051	0.0087	0.0023	***0.00099***
SNR	1.8052	8.7419	6.4030	12.2398	***16.1116***
Cross-correlation	0.7400	0.9350	0.8881	0.9697	***0.9879***

Table 4.6: Results for Simulated ECG with *Noise 6*
SNR (input) = 2.2903; MSE(noisy) = 0.0226

	Using Wavelet		Only EMD	Only Morphological	Our Algorithm
	HT	ST			
MSE	0.0088	0.0034	0.0033	0.0013	***0.00081***
SNR	6.3795	10.5084	10.6047	14.8282	***16.7256***
Cross-correlation	0.8888	0.9548	0.9559	0.9835	***0.9894***

Following graphs, shows the proposed algorithm for the simulated ECG corrupted with *noise 1*.

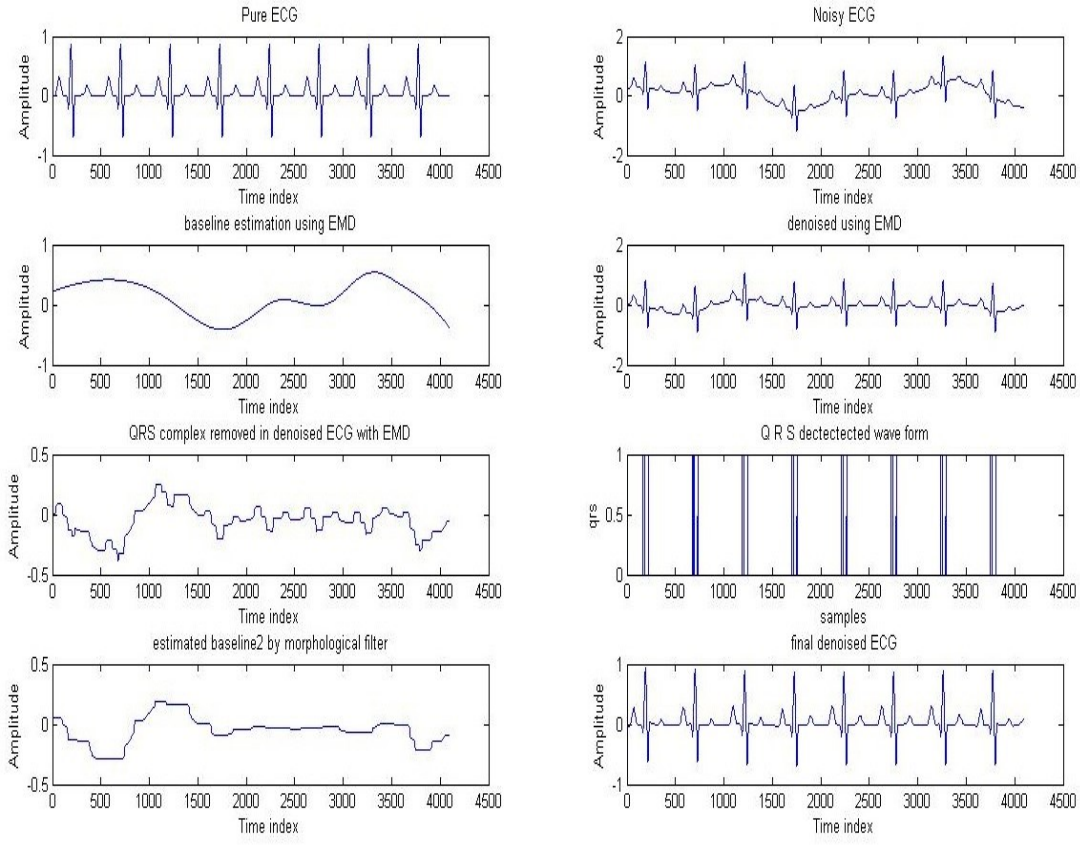

Fig 4.4: Results for Simulated ECG: corrupted with *Noise1*

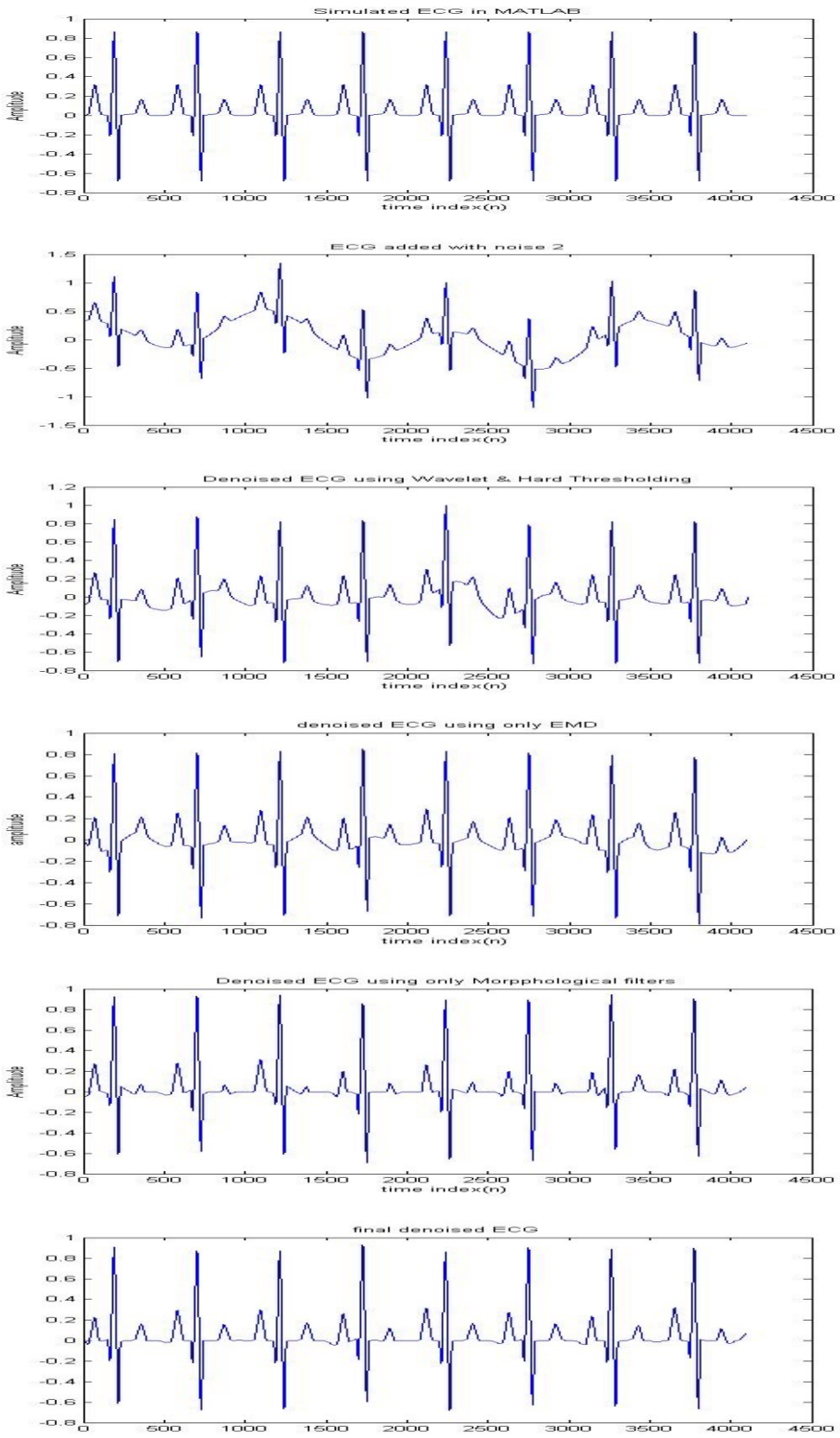

Fig 4.5: Comparative results: (from top to bottom) (a) pure ECG (b) noisy ECG (c) denoised using wavelet & hard thresholding (d) denoised using EMD only (e) denoised using only Morphological method (f) denoised using novel technique

4.5 Simulation Results for Real ECG

For the purpose of testing our algorithm against real ECG data, it is important to perform the denoising operation over a real data. The major challenge in the implementation of algorithm for real ECG, is in quantification of results because of the pre-existing noise which adds to the real data at the time of signal acquisition. One such database was discovered at physiobank database, named ECG-ID Database (ecgiddb) which has both raw ECG data and filtered ECG data. So, filtered ECG data are used for simulation and compilation of results.

Following figure shows the denoising of a real ECG signal taken from ecgiddb: signal person_03/rec_02.

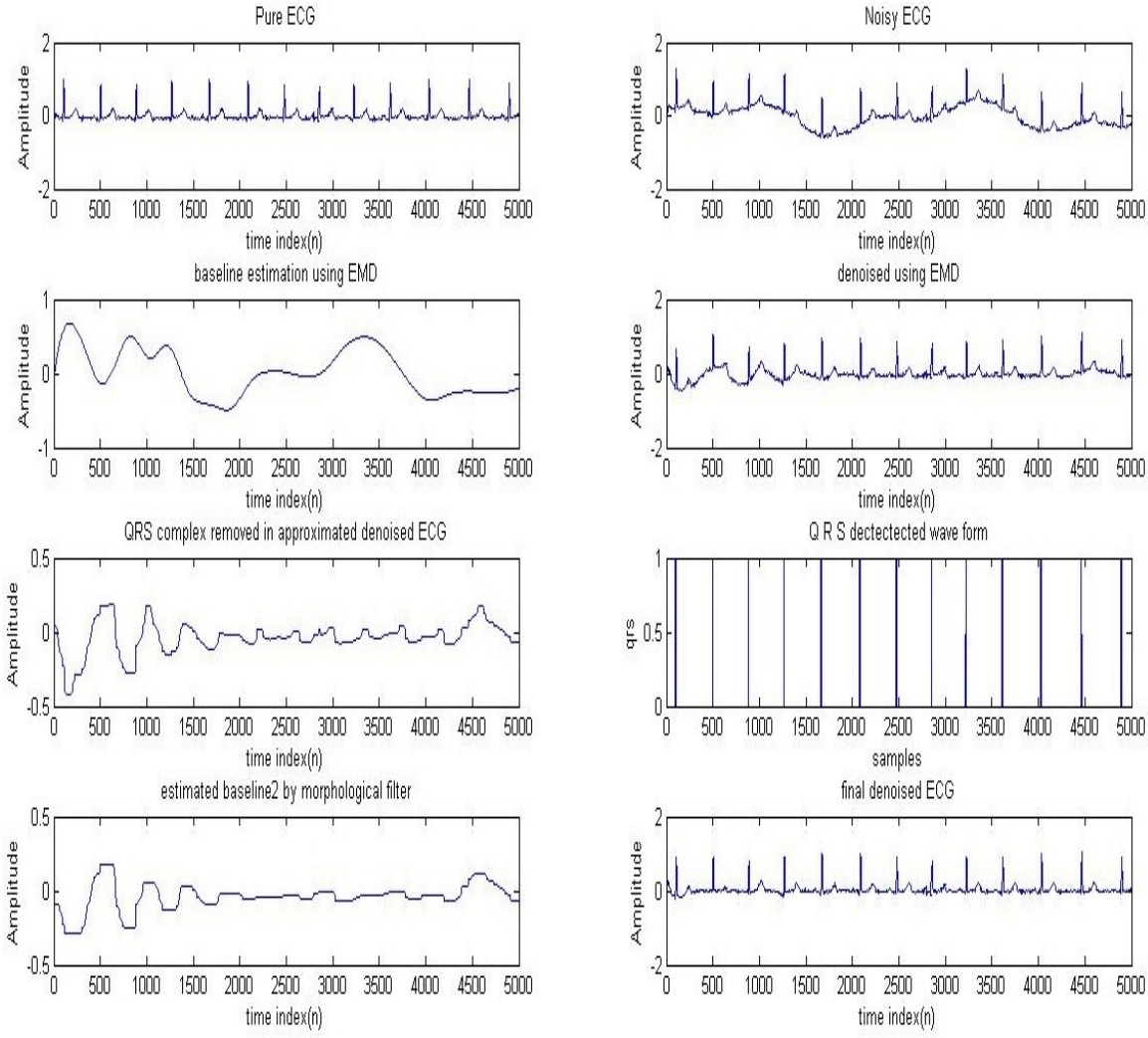

Fig 4.6: Results for real ECG signal person_03/rec_02 (ecgiddb)

In a similar way, as explained in above section for synthetic ECG (Figure. 4.3), the Fig. 4.4 represents the steps in denoising for a real ECG signal. While the first graph in Fig. 4.4 is real ECG signal taken from ECG-ID Database. The noise added here is *Noise 1* as described in the above section. As evident from, *graph 4* EMD is unable to remove the baseline drift completely, hence the approximate corrected ECG is then filtered with morphological filters to completely eliminate the baseline drift noise.

In a similar manner, this denoising algorithm is executed with different real ECG signals taken from the same database to check for the robustness of the chosen structuring element. The results are compiled in a tabular form as below:

Table 4.7: Comparison of SNR improvement by conventional SE and modified SE for real ECG with different heart rates.

Input ECG (ECG-ID Database)	Heart Rate	SNR improvement by conventional structuring element	SNR improvement by modified structuring element
Person_03/rec_2	70	13.3453	14.1052
Person_17/rec_2	57.5	16.1774	16.8521
Person_01/rec_5	67.5	12.0948	12.3932
Person_08/rec_1	77.5	13.1512	13.7185

Figure below, shows another real ECG data of person_17/recording_02 denoised using the novel algorithm:

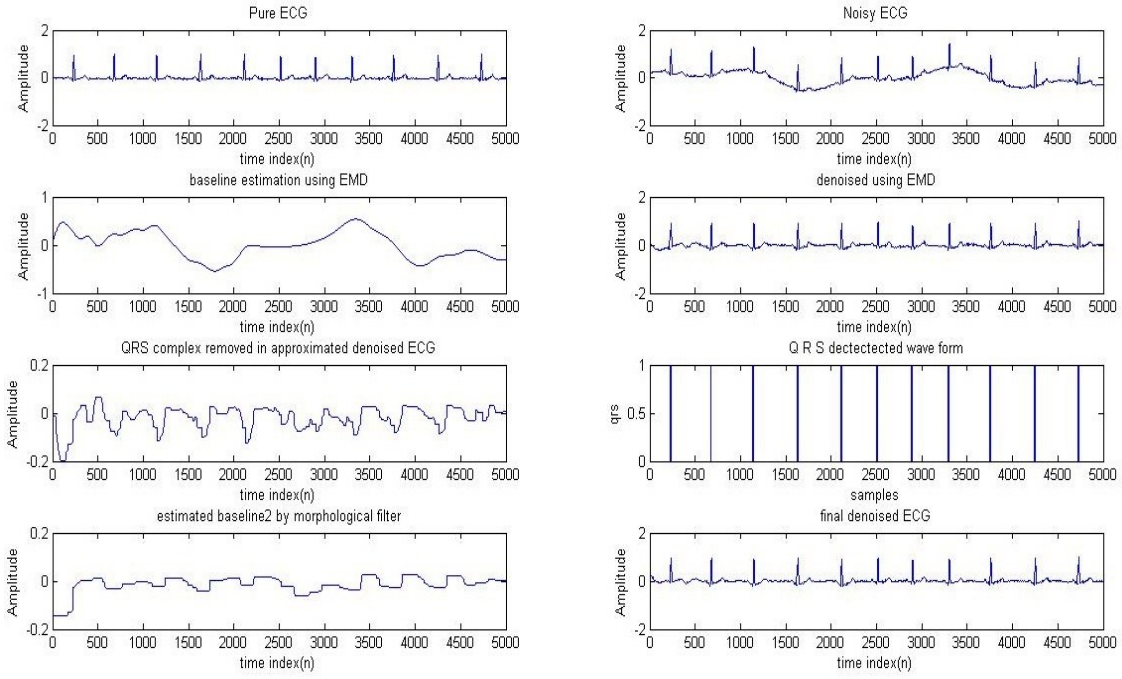

Fig 4.7: Results for real ECG signal person_17/recording_02.

Chapter 5

CONCLUSION AND FUTURE SCOPE

In this chapter, final conclusions are drawn on the basis of the results. The limitations of the existing algorithms and the future scope of the proposed work are also elaborated.

5.1 Conclusion

This thesis work, throws light on the denoising of the ECG signals. Starting with the basics of electrocardiogram, the type of noises that are added with the ECG signal at the time of signal acquisition and the basics of ECG morphology all parts were thoroughly covered, followed by a very comprehensive Literature review, in which most of the earlier efforts are examined in detail. The inefficiency of wavelet transforms in the denoising of baseline noise is brought into notice.

A hybrid model is proposed in this work, in which empirical mode decomposition and morphological filters are cascaded. The structuring element of the morphological filters has been modified so as to make the proposed algorithm partially adaptive. The algorithm is said to be partially adaptive because only the structuring element for morphological filtering phase-II has been adaptively derived from the data while the structuring element for morphological filters phase-I has been set according to the theoretically known duration of the QRS complex from medical sciences as the duration of the QRS complex is almost independent of the heartbeat.

The proposed method is tested against wavelet transform, only EMD and only morphological filtering. As observed in Table 4.1 to 4.6, wavelet transform gives inconsistent results with the varying frequency. Also the results are varying between hard thresholding and soft thresholding. For some frequency of noise hard thresholding performed better while for others soft thresholding gave better results. Thus a particular threshold cannot be optimally selected with the wavelet to obtain good results for baseline correction. Hence, wavelet transforms is not a good tool for baseline correction. This is because the wavelet is a time-frequency dependent transform and as the noise frequency varies the results also varies. As is also seen from the fig 4.4, baseline correction using

wavelet transform does not give good results and the ST segment is heavily distorted due to the presence of baseline drift.

Baseline correction using empirical mode decomposition is better than that of wavelet transforms as the decomposition is not a function of time-frequency but is a function of the local variations present in the signal. Hence, the results for denoising using EMD are consistent with the varying frequency. All the smaller variations are left in the higher order IMFs but generally smaller variations in ECG signals (low frequency information content) also gets added to some of the IMFs. Thus, this overlapping does not allows complete elimination of the baseline drift. Hence, EMD alone without any processing of the IMFs cannot be used for baseline correction.

Morphological filtering is independent of any time-frequency information of the data. It is simply related with the morphology of the input signal. Hence, among all the suggested algorithms in the literature so far, morphological filters is the finest algorithm for removal of baseline noise from the signal. But again if a data heavily corrupted by baseline noise is directly fed into morphological filter, the finer variations in the baseline are not removed. Hence, an input with relatively low baseline noise component is denoised very nicely, and very fine variations present in the baseline are also detected and removed.

Thus, the proposed algorithm shows very good results for baseline correction. A correlation coefficient as high as 0.99 is achieved using the proposed algorithm, which is far more than that achieved using other techniques for same noise level. The proposed algorithm is simulated over synthetic ECG, generated in MATLAB and also real ECG signal. For the synthetic ECG quantification of the results is done properly because of the availability of 100% pure signal. For synthetic ECG signal, SNR improvement of as high as 19.45 db is obtained which is very high compared to 14.91 db obtained using morphological filters (the closest to the proposed algorithm among all others). For testing of the modified structuring element used in the proposed algorithm real ECG signal is used from ECG-ID Database. Consistently, in spite of varying heart rate the proposed algorithm with adaptive SE gave better results compared to the hybrid algorithm with conventional SE.

This proposed algorithm, with adaptive SE is expected to perform even better for exercise ECGs or ECGs recorded at higher heart rate because of the induced upward slope of ST

interval at high heart rate. This upward sloping with increase in heart rate can be effectively managed by the adaptive SE which is a function of the heart rate.

5.2 Future Scope

Though a lot of efforts has been put in to build this algorithm optimally, but some developments can still be made to this work as follows:

- Making the algorithm completely adaptive and choosing the QRS complex also from the data itself.
- Preprocessing of the IMFs being deleted can be done to further enhance the results.
- An adaptive approach for estimation of noisy IMFs can be formulated to improve the performance.
- Synthesis of high heart rate ECG signals, which are originally 100% pure can be used for better compilation of results at higher heart rates.

REFERENCES

[1] I Mervin and J. Goldman, "The Principles of Clinical Electrocardiography", Los Altos, Calif.: Lange Medical Publications, 1992.

[2] J. Moss and S. Stern., "Non-invasive electro cardiology: Clinical aspects of holter monitoring", 1st edition, 1996, W.B. Saunders, Philadelphia, ISBN: 9-7020-1925-9.

[3] M. Gabriel Khan, "Rapid ECG Interpretation", 3rd edition, 2008, Humana press, New York, ISBN- 978-1-58829-979-6.

[4] S.K. Jagtap, M.S. Chavan, R.C. Wagvekar and M.D. Uplane, "Application of the digital filter for noise reduction in electrocardiogram". Journal of Instrumentation, vol.40, no. 2, pp. 83–86, June 2010.

[5] Dr. K. L. Yadav and Sachin Singh, "Performance evaluation of different adaptive filters for ECG signal processing", International Journal On Computer Science and Engineering, vol. 40, no. 5, pp. 1880–1883, 2010.

[6] Muhammad ZiaUrRahman, Rafi Ahamed Shaik and D.V.RamaKoti Reddy, "Efficient sign based normalized adaptive filtering techniques for cancelation of artifacts in ECG signals: Application to wireless biotelemetry", Journal of signal processing, vol. 91, no. 2, pp. 225–239, February 2011.

[7] Ching-Haur Chang ,Kang-Ming Chang ,and Hsien-Ju Ko, "Cancellation of high frequency noise in ECG signals using Adaptive filter without external reference", Proceedings of International Conference on Biomedical Engineering and Informatics, pp. 787–790, Yantai, October 2010.

[8] Y. Der Lin and Y. Hen Hu, "Power-line interference detection and suppression in ECG signal processing," IEEE Trans. Biomed. Eng., vol. 55, pp. 354-357, Jan.2008.

[9] N. V. Thakor and Y. S. Zhu, "Applications of adaptive filtering to ECG analysis: noise cancellation and arrhythmia detection," IEEE Transactions on biomedical engineering vol. 18. No. 8. August 1991.

[10] S.Z.Islam, R.Jidin, M.Ali, "Performance Study of Adaptive Filtering Algorithms for Noise Cancellation of Electrocardiogram (ECG) Signal" 7th International Conference on Information, Communications and Signal Processing, 2009. IEEE ICICS 2009, pp. no: 1-5, 2009.

[11] Omid Sayadi and Mohammad Bagher Shamsollahi, "Electrocardiogram (ECG) De-noising and Compression Using a Modified Extended Kalman Filter Structure ", IEEE Transactions on Biomedical Engineering, Vol. 55, No. 9, pp.no: 1064-1068, 2008.

[12] C.Y.-F Ho, B.W.-K, Ling, T.P.-L. Wong, A.Y.-P. Chan, P.K.-S.Tam, "Fuzzy rule based multi-wavelet Electrocardiogram (ECG) de-noising", Fuzzy Systems, IEEE International Conference , pp. no 1064-1068, 2008.

[13] K. Barros, A. Mansour and N. Ohnishi, “Removing artifacts from electrocardiographic signals using independent components analysis”, Journal of Neuro-computing, vol. 22, no. 1–3, pp. 173–186, 1998.
[14] T. He, G. D. Clifford, and L. Tarassenko, “Application of independent component analysis in removing artefacts from the electrocardiogram,” Journal of Neural Computing Applications, vol. 15, no. 2, pp. 105–116, 2006.
[15] G. B. Moody and R. G. Mark, “QRS morphology representation and noise estimation using the Karhunen-Loeve transform”, Proceedings of International conference on Computers in Cardiology, pp. 269–272, Jerusalem, Israel, September 1989.
[16] G. D. Clifford, L. Tarassenko and N. Townsend, “One-pass training of optimal architecture auto-associative neural network for detecting ectopic beats”, Electronics letters, vol. 37, no. 18, pp. 1126-1127, August 2001.
[17] DL Donoho, “De-noising by soft-thresholding”, IEEE Trans Inform Theory, 14(3), 1995, pp. 612-627.
[18] M. Alfaouri and K. Daqrouq, "Electrocardiogram (ECG) Signal Denoising by Wavelet Transform Thresholding", American Journal of Applied Sciences, Vol. 5 Issue: 3, pp. no 276-281, 2008
[19] M Kania, M Fereniec, R Maniewski, "Wavelet De-noising for Multilead High Resolution Electrocardiogram (ECG) Signals", Measurement Science Review, Volume 7, Section 2, No. 4, pp. no 30 - 33,2007.
[20] L. Chmelka and J. Kozumplik, "Wavelet-Based Wiener Filter for Electrocardiogram Signal De-noising", IEEE Computers in Cardiology 2005, pp. no: 771-774, 2005.
[21] I.M. Johnstone, B.W. Silverman, "Wavelet threshold estimators for data with correlated noise", J. R. Statist. Soc. Ser. B vol.59, 1997, pp.319–351.
[22] A.G. Bruce and H.Y. Gao, "Understanding Wave Shrink: Variance and bias estimation", Biometrika (1996), 83.4, pp. 727-745.
[23] Yang Ying, "ECG signals denoising using neighboring Coefficients", IEEE Bioinformatics and Biomedical Engineering, (ICBBE) 2011 5th International Conference on 10-12 May, 2011.
[24] Mozaffary and M. A. Tinati, “ECG Baseline Wander Elimination using Wavelet Packets”, World Academy of Science, Engineering and Technology, Vol. 3, 2005, pp. 14-16.
[25] J.S. Sahambi, S.N. Tandon, R.K.P. Bhatt, “Using Wavelet Transform for ECG Characterization”, IEEE Engineering in Medicine and Biology Magazine, January/February 1997 issue, pp. 77─84.
[26] D.T Luong, "Study on the limitations of removal of baseline noise from electro cardiography signal in measurement using wavelet analysis ", IEEE, ICUFN, 2013.
[27] A.O. Boudraa, J.-C. Cexus,"EMD-Based Signal Filtering," IEEE Transactions on instrumentation and Measurement, vol. 56, no. 6, pp.2196-2202, Dec. 2007.

[28] Anil Chacko and Samit Ari, “Denoising of ECG signals using Empirical Mode Decomposition based technique” IEEE-International Conference On Advances In Engineering, Science And Management (lCAESM -2012) March 30, 31, 2012 pg no.6-9.

[29] Yan Lu, Jingyu Yan, and Yeung Yam, “Model-based ECG Denoising Using Empirical Mode Decomposition”, 2009 IEEE International Conference on Bioinformatics and Biomedicine pg no. :191-196.

[30] B.Pradeep Kumar, S. Balambigai and R. Asokan, "ECG De-Noising Based On Hybrid Technique", IEEE-International Conference on Advances In Engineering, Science And Management (ICAESM -2012), pp. no: 285-290, 2012.

[31] Changnian Zhang, XiaLi and Mengmeng Zhang, “A novel ECG signal denoising method based on Hilbert-Huang Transform”, 201O International Conference on Computer and Communication Technologies in Agriculture Engineering, CCTAE-2010 pg no: 284-287.

[32] Zhi-Dong Zhao, Yu-Quan Chen, “A New Method for Removal of Baseline Wander and Power Line Interference in ECG Signals”, Proceedings of the Fifth International Conference on Machine Learning and Cybernetics, Dalian, 13-16 August 2006 , pg no.: 4342-4347.

[33] Na Pan, Vai Mang I, Mai Peng Un and Pun Sio hang, “Accurate Removal of Baseline Wander in ECG Using Empirical Mode Decomposition”, Proceedings of NFSI & ICFBI 2007 Hangzhou, China, October 12-14, 2007, pg no.: 177-180.

[34] Chee-Hung Henry Chu and Edward J. Delp,“Impulsive Noise Suppression and Background Normalization of Electrocardiogram Signals Using Morphological Operators”, IEEE Transactions on Biomedical Engineering. Vol. 36, No. 2, February, 1989, pg no. 262-273.

[35] Seyfullah Halit OGUZ and Musa Hakan ASYALI, “A Morphology based Algorithm for Baseline Wander Elimination in ECG records”, International Biomedical Engineering days, 1992, pg no. 157-160.

[36] P. Sun, Q. H. Wu, A. M. Weindling, A. Finkelstein, and K. Ibrahim, “An Improved Morphological Approach to Background Normalization of ECG Signals”, IEEE Transactions on Biomedical Engineering, Vol. 50, No. 1, January, 2003, pg no.: 117-121.

[37] Zhongguo Liu, Jinliang Wang and Boqiang Liu, “ECG Signal Denoising Based on Morphological Filtering”, 5th International Conference on Bioinformatics and Biomedical Engineering, (iCBBE) 2011.

[38] R.J. Gibbons et al., “Guideline update for exercise testing: A report of the ACC/AHA task force on Practice Guidelines (committee on exercise testing),” Journal of American College of Cardiology, pg. 6, Elsevier 2002.

[39] M.L. Ahlstrom and W.J. Tompkins, “Automated high-speed analysis of holter tapes with microcomputers,” IEEE Trans. Biomed. Eng., vol. 30, pp. 651-657, Oct. 1983.

[40] J. Fraden and M.R. Neumann, “QRS wave detection,” Med. Biol. Eng. Comput., vol. 18, pp. 125-132, 1980.
[41] P.O. Börjesson, O. Pahlm, L. Sörnmo, and M.-E. Nygards, “Adaptive QRS detection based on maximum a posteriori estimation,” IEEE Trans. Biomed. Eng., vol. 29, pp. 341-351, May 1982.
[42] T. Fancott and D.H. Wong, “A minicomputer system for direct high-speed analysis of cardiac arrhythmia in 24 h ambulatory ECG tape recordings,” IEEE Trans. Biomed. Eng., vol. 27, pp. 685-693, Dec. 1980.
[43] V. Di-Virgilio, C. Francaiancia, S. Lino, and S. Cerutti, “ECG fiducial points detection through wavelet transform,” in 1995 IEEE Eng. Med. Biol. 17th Ann. Conf. 21st Canadian Med. Biol. Eng. Conf., Montreal, Quebec, Canada, 1997, pp. 1051-1052.
[44] C. Li, C. Zheng, and C. Tai, “Detection of ECG characteristic points using wavelet transforms,” IEEE Trans. Biomed. Eng., vol. 42, pp. 21-28, 1995.
[45] S. Kadambe, R. Murray, and G.F. Boudreaux-Bartels, “Wavelet transform-based QRS complex detector,” IEEE Trans. Biomed. Eng., vol. 46, pp. 838-848, 1999.
[46] V.X. Afonso, W.J. Tompkins, T.Q. Nguyen, and S. Luo, “ECG beat detection using filter banks,” IEEE Trans. Biomed. Eng., vol. 46, pp. 192-202, 1999.
[47] D.A. Coast, R.M. Stern, G.G. Cano, and S.A. Briller, “An approach to cardiac arrhythmia analysis using hidden Markov models,” IEEE Trans. Biomed. Eng., vol. 37, pp. 826-836, 1990.
[48] S.-K. Zhou, J.-T. Wang, and J.-R. Xu, “The real-time detection of QRS-complex using the envelop of ECG,” in Proc. 10th Annu. Int. Conf.,IEEE Engineering in Medicine and Biology Society New Orleans, LA, 1988, p. 38.
[49] Bert-Uwe Köhler, Carsten Hennig and Reinhold Orglmeister, “The Principles of Software QRS Detection” IEEE Engineering in Medicine and Biology, January/Feburary, 2002. Pg no.: 42-57.
[50] N. E. Huang, Z. Shen, S. R. Long, M. e. Wu, H. H. Shih, Q. Zheng, N. e. Yen, e. e. Tung, and H. H. Liu, "The empirical mode decomposition and the Hilbert spectrum for nonlinear and nonstationary time series analysis," Proc. Roy. Soc. Lond. A, Math. Phys. SCi., vol. 454, pp. 903-995, Mar. 1998.
[51] Trahanias, P.E, “An approach to QRS complex detection using mathematical morphology,” J. IEEE Trans Biomed Engg, vol.40, pp.262–272, 1993.
[52] Book: “Hilbert-Huang transform and its applications” by Norden E Huang and Samuel S P Shen, Chapter 1: Introduction to Hilbert Huang Transform and its related Mathematical problems. World Scientific Publishing Co. Ltd.
[53] Book: “Digital Image Processing” by Rafael C. Gonzalez, Pearson education India, 2009, Chapter 9: Morphological Image Processing, pp no. 649.
[54] C. L. Luengo Hendriks, L.J. Van Vliet, “Using Line Segments as Structuring Elements for Sampling-Invariant Measurements,” J. IEEE Transaction on Pattern Analysis and Machine Intellingnce,2005,vol.27,no.11,pp.1826-1831,2005.

[55] J.Pan and W.J. Tompkins“A Real-Time QRS Detection Algorithm”, IEEE Transactions on Biomedical Engineering, Vol. BME-32, No. 3, March, 1985.
[56] Book: “Practical ECG for Exercise Science and Sports Medicine”, by Greg Whyte and Sanjay Sharma.
[57] Goldberger AL, Amaral LAN, Glass L, Hausdorff JM, Ivanov PCh, Mark RG, Mietus JE, Moody GB, Peng C-K, Stanley HE. PhysioBank, PhysioToolkit, and PhysioNet: Components of a New Research Resource for Complex Physiologic Signals. *Circulation* 101(23):e215-e220; 2000 (June 13).
[58] Lugovaya T.S. Biometric human identification based on electrocardiogram. [Master's thesis] Faculty of Computing Technologies and Informatics, Electrotechnical University "LETI", Saint-Petersburg, Russian Federation; June 2005.

APPENDICES

Appendix – I

In the tables A-1 to A-3, the comparative results of different wavelets and thresholding technique for three possible different noises are compiled.

Table A-1: Output SNR in denoised ECG in case of Powerline Interference Noise (Input SNR = 8.0437 dB)

Thresholding / Wavelet	Hard	Soft	Semi-soft	Stein	NE
Haar	11.0631	11.4889	11.4895	10.3383	14.3268
Db5	11.9387	19.1262	19.1265	17.4667	12.7945
Coif3	10.1017	19.2341	19.2342	16.5323	12.5641
Bior3.1	9.4413	13.0481	13.0490	11.5702	11.4507
Db4	10.3578	19.9982	19.9986	17.7033	12.7656
Sym8	10.2601	20.8799	***20.8806***	19.1266	12.4789
Sym10	11.1715	20.3877	20.3882	18.3906	12.5524
Bior6.8	10.9729	20.4565	20.4573	18.4721	12.4772
Db6	11.7305	20.4982	20.4985	18.8580	12.7532
Coif4	9.9168	20.8490	20.8499	19.0435	12.4336

Table A-2: Output SNR in denoised ECG in case of Baseline Drift Noise (Input SNR = –2.4526 dB)

Thresholding / Wavelet	Hard	Soft	Semi-soft	Stein	NE
Haar	2.0808	6.0234	6.0238	6.0278	5.4726
Db5	3.2726	8.7624	10.5035	9.0564	4.6949
Coif3	3.5440	7.6518	11.1640	4.7805	4.3106
Bior3.1	3.5462	9.1473	11.2209	10.6766	4.4560
Db4	4.7123	6.6061	10.3418	3.6177	2.8443
Sym8	4.8903	6.3779	12.4014	2.2835	3.4155
Sym10	5.0004	6.0479	***12.5427***	1.9325	3.2476
Bior6.8	4.8951	7.3764	11.4303	4.0869	4.1252
Db6	3.2855	9.5187	11.3540	9.5994	4.9697
Coif4	5.0092	7.3531	11.4993	3.8982	4.0011

Table 6: Output SNR in denoised ECG in case of Wideband Stochastic Noise/EMG Noise (Input SNR = 6.1817 dB)

Thresholding / Wavelet	Hard	Soft	Semi-soft	Stein	NE
Haar	10.8378	10.4503	10.6720	10.0344	12.2022
Db5	14.3871	14.3873	14.3877	13.8203	14.4354
Coif3	14.4541	14.4348	14.4348	13.7311	14.5024
Bior3.1	8.8339	8.8895	8.8899	8.2269	9.9710
Db4	14.6813	14.7270	14.7272	13.9550	14.7367
Sym8	14.8125	14.8805	14.9015	14.1674	14.9112
Sym10	14.6565	14.8566	14.8566	14.1133	***14.9125***
Bior6.8	14.6840	14.8837	14.8840	14.1553	14.9004
Db6	14.6376	14.8371	14.8376	14.1353	14.8376
Coif4	14.6459	14.8885	14.8888	14.1541	14.8894

Appendix – II

The following is the excerpt taken from the book "Practical ECG for Exercise Science and Sports Medicine", by Greg Whyte and Sanjay Sharma. This excerpt is helpful in understanding the important changes in the morphology of the heart for post-exercise ECG records and thus selecting the length of SE2.

Expected ECG Changes in the Normal Heart

The altered action potential duration, conduction velocity, and contractile velocity associated with the increase in heart rate during exercise results in a number of ECG changes in normal people, including the following:

- RR interval decreases.
- P-wave amplitude and morphology undergo minor changes.
- Septal Q-wave amplitude increases.
- R-wave height increases from rest to submaximal exercise and then reduces to a minimum at maximal exercise.
- The QRS complex experiences minimal shortening.
- J-point depression occurs.
- Tall, peaked T waves occur (high interindividual variability).
- **ST segment becomes upsloping.**
- QT interval experiences a rate-related shortening.
- Superimposition of P waves and T waves on successive beats may be observed.

Heart Rate (in bpm)	QT duration (in ms)
60	330-430
80	290-380
100	270-350
120	250-320
140	230-280
160	210-260
180	190-240